W. Chen et al. *Res Math Sci(2020)7:13*
https://doi.org/10.1007/s40687-020-00212-9

Research in
the Mathematical Sciences

RESEARCH

Energy stable higher-order linear ETD multi-step methods for gradient flows: application to thin film epitaxy

Wenbin Chen[1], Weijia Li[2], Cheng Wang[3], Shufen Wang[2] and Xiaoming Wang[4*]

*Correspondence:
wangxm@sustech.edu.cn
[4]SUSTech International Center for Mathematics and Department of Mathematics, Southern University of Science and Technology, Shenzhen 518055, People's Republic of China
Full list of author information is available at the end of the article

Dedicated to Professor Andrew Majda on the occasion of his seventieth birthday.

Abstract

We discuss how to combine exponential time differencing technique with multi-step method to develop higher order in time linear numerical scheme that are energy stable for certain gradient flows with the aid of a generalized viscous damping term. As an example, a stabilized third order in time accurate linear exponential time differencing (ETD) scheme for the epitaxial thin film growth model without slope selection is proposed and analyzed. An artificial stabilizing term $A\tau^3 \frac{\partial \Delta^3 u}{\partial t}$ is added to ensure energy stability, with ETD-based multi-step approximations and Fourier pseudo-spectral method applied in the time integral and spatial discretization of the evolution equation, respectively. Long-time energy stability and an $\ell^\infty(0, T; \ell^2)$ error analysis are provided, based on the energy method. In addition, a few numerical experiments are presented to demonstrate the energy decay and convergence rate.

Keywords: Gradient flow, Epitaxial thin film growth, Exponential time differencing, Long-time energy stability, Convergence analysis, Third-order scheme

Mathematics Subject Classification: 65M12, 65M70, 65Z05

1 Introduction

Numerical schemes that preserve certain structures/properties for the underlying system are highly desirable since these schemes usually perform better in terms of capturing certain behavior of the models under approximation when compared to classical methods. Well-known examples include absorbing boundary condition method for acoustic and elastic wave equations in the whole space [19], symplectic integrator for Hamiltonian systems [21], SSP and TVD for hyperbolic conservation laws [26], dispersion relation preserving schemes for the acoustic equations [52], asymptotic preserving schemes for the kinetic equations [31], and energy stable schemes for gradient flows, the focus of this paper, among many others.

The desire to derive energy stable schemes for gradient flows is obvious since the energy law is usually the most prominent property of the PDE system. In addition, for gradient flows such as thin film epitaxial growth models, the coarsening process, which succeeds the relatively fast phase separation process, occurs on a very long-time scale for large systems (or small parameter ε as shall be introduced below). Stability is of particular importance for such kind of long-time numerical approximations, and an appropriate energy law of the scheme that mimics the energy law of the original system would certainly be very beneficial in ensuring the stability of the simulation among others.

A variety of techniques exist for developing energy stable schemes for gradient flows such as convex splitting [20,53], invariant energy quadratization method (IEQ) [56], scalar auxiliary variable (SAV) method [51].

On the other hand, accuracy order is another highly desirable issue. To seek higher order in time algorithms, exponential time differencing (ETD) seems to be a very effective way to minimize time discretization errors [29]. The basic idea of ETD is to utilize the solution operator of the linear evolutionary equation without truncation. Since ETD cannot be applied to nonlinear equations alone, a natural idea is to combine ETD with other methods that can be used to efficiently approximate the nonlinear part, and multi-step method is one of the natural candidates for such approximations [28]. The other natural choice is the Runge–Kutta method; see [29] for ETD-RK approaches. The nonlinear term is customary treated explicitly for efficiency in the ETD-MS approach. However, such an explicit treatment may induce instability. Application of the ETD-MS method to epitaxial growth model without slope selection can be found in [32] among others. Meanwhile, the stability of these ETD-MS is non-trivial due to the instability induced by the explicit treatment of the nonlinear term. Unconditionally stable second-order ETD-MS is derived only recently with an artificial stabilizing term [9]. See also [14] for a slightly different approach in terms of stabilization.

The main contribution of this paper is to formulate a general strategy for the development of efficient energy stable higher-order linear ETD-MS algorithms for certain gradient flows. A key ingredient of the strategy is an appropriate stabilization term which could be interpreted as a higher-order viscous term. Roughly speaking, for an evolutionary equation of the form

$$\frac{\mathrm{d}u}{\mathrm{d}t} + Lu = N(u),$$

where L is a positive operator and N is a nonlinear operator, we apply the ETD-MS method to

$$\frac{\mathrm{d}u}{\mathrm{d}t} + Lu + A\tau^k \frac{\mathrm{d}}{\mathrm{d}t} L^{p(k)} u = N(u),$$

in order to derive a kth order energy stable scheme with time-step size τ and appropriate choice of exponent $p(k)$. The term $A\tau^k \frac{\mathrm{d}}{\mathrm{d}t} L^{p(k)} Lu$ can be interpreted as a higher-order viscous regularization part; see the Cahn–Hilliard case [43]. The artificial viscous term is kept in the continuum version which is consistent with the spirit of ETD method. Explicit treatment of the nonlinear term is desirable for efficiency consideration. However, higher-order multi-step treatment of the nonlinear term leads to strong instability which requires a higher-order artificial viscous term to stabilize the scheme. This stabilization term could be understood as a continuum version of classical Dupont–Douglas type regularization. Special care is needed for the explicit treatment of the nonlinear part, even with the stabilization term, in order to ensure energy stability. Lagrangian approach seems to be an appropriate choice in this case. We would need the nonlinear term to be "not too bad" for such an explicit treatment to work out. We are not sure whether our approach works for systems with stronger nonlinear term such as epitaxial growth model with slope selection.

As a specific example, we consider the following epitaxial growth model without slope selection. We offer a third-order energy stable ETD-MS scheme for this model. The energy stability as well as the third-order convergence analysis will be presented.

Consider the following nonlinear diffusion equation that models no-slope-selection epitaxial growth:

$$\frac{\partial u}{\partial t} = -\varepsilon^2 \Delta^2 u - \nabla \cdot \left(\frac{\nabla u}{1 + |\nabla u|^2} \right), \ x \in \Omega, \ t \in (0, T], \tag{1}$$

where $\Omega = [0, L]^2$, $u : \Omega \times [0, T] \to \mathbb{R}$ is a scaled height function of thin film with periodic boundary condition, and $\varepsilon > 0$ is a constant. Due to the periodic boundary condition, the solution $u(\mathbf{x}, t)$ is mass conservative, namely $\int_\Omega u(\mathbf{x}, t)\, \mathrm{d}\mathbf{x} = \int_\Omega u(\mathbf{x}, 0)\, \mathrm{d}\mathbf{x} = 0$.

In this case, $L = \varepsilon^2 \Delta^2, N(u) = -\nabla \cdot \left(\frac{\nabla u}{1+|\nabla u|^2} \right)$ in our general framework. The exponent in the regularization term will be $p(3) = 3/2$, as we shall see below.

The equation (1) turns out to be the L^2 gradient flow of the following energy functional:

$$E(u) = \int_\Omega \frac{\varepsilon^2}{2} |\Delta u|^2 - \frac{1}{2} \ln(1 + |\nabla u|^2)\, \mathrm{d}\mathbf{x}, \tag{2}$$

where the first term represents the surface diffusion, and the logarithm term models the Ehrlich–Schwoebel (ES) effect which describes the effect of kinetic asymmetry in the adatom attachment–detachment; see [18,37,38,48] for more detailed descriptions.

The reason why this model is referred as "no-slope-selection"(NSS) is based on the fact that (1) predicts a time-dependent mound slope $m(t) = O(t^{\frac{1}{4}})$ before saturation [24,38]. On the other hand, with the ES effect term in $E(u)$ replaced by $\frac{1}{4}(|\nabla u|^2 - 1)^2$, the corresponding growth equation is called slope-selection (SS), which predicts a uniform, constant mound slope for the mound-like structures in the surface profile. Well-posedness of the initial-boundary-value problem for both SS and NSS equations has been given by [37,38] through the perturbation analysis and Galerkin spectral approximations.

In the epitaxial growth model field, scaling laws of the energy E, the average surface roughness $h(t) = \frac{1}{\sqrt{|\Omega|}} \|u(\cdot, t)\|$ and the average slope $m(t) = \frac{1}{\sqrt{|\Omega|}} \|\nabla u(\cdot, t)\|$ have been physically interesting quantities, and it is generally accepted that $E \sim O(-\ln t)$, $h(t) \sim O(t^{\frac{1}{2}})$ and $m(t) \sim O(t^{\frac{1}{4}})$; see [24,36,37,39,44]. The coarsening process is expected to scale like L^4 for the NSS case (L^3 for the SS case) which is long for large system (large L) [38]. Hence, long-time energy stability is needed to accurately simulate the coarsening process.

One popular way to construct energy stable numerical schemes is to split the energy functional into convex and concave parts and apply implicit and explicit treatments [20], respectively; the first such numerical scheme for the molecular epitaxy growth model is proposed in [53]. Since then, there have been various works applied to the epitaxial growth equation under this framework, such as [8,10,12,42,45,46,50]. On the other hand, the splitting approach is known to have difficulty in constructing unconditionally stable higher-order schemes for a nonlinear concave term. To overcome this subtle difficulty, one prevalent approach is to introduce an artificial stabilizing term in the growth equation, which balances the explicit treatment of the nonlinear term; see [22,40,41,55]. In addition, there have been some other interesting energy stable approaches, such as the invariant energy quadratization (IEQ) [56] and the scalar auxiliary variable (SAV) methods [16,51], etc.

Other than the approaches mentioned above, another idea to obtain higher-order temporal accuracy while explicitly computing nonlinear terms is the time exponential time differencing (ETD) method. In general, the ETD-based scheme contains an exact integration of the linear part of the NSS equation, with the temporal integral of the nonlinear term approximated by multi-step explicit approximation [3,4,17,29,30]. Applications of such an idea to various gradient flow models have been reported in recent works [14,32–35,54,57], with the high order accuracy and preservation of the exponential behavior observed in the numerical experiments. In particular, the energy stability analysis for the first-order (in time) scheme is established in [32]; the one for the second-order scheme is reported in a more recent work [9]. Generalizing the idea from [9,14] presents a third order in time ETD-based scheme for the no-slope-selection model, in which $A\tau^2\Delta_N^2(u^{n+1}-u^n)$ (with τ the time step size) is added as the stabilization term with $A=O(\varepsilon^{-2})$.

In this article, we propose another third order in time accurate energy stable ETD-based scheme, with Fourier pseudo-spectral approximation in space, which avoids the singular dependence on the coefficient in the regularization term in terms of ε. Following the idea in [9], an artificial stabilizing term $A\tau^3\frac{\partial\Delta^3 u}{\partial t}$ is added in the growth equation, where A is a positive constant independent of ε. In addition, we apply a three level Lagrange approximation to the nonlinear term. This approach enables us to derive a decay property for a modified discrete energy functional, which in turn leads to a uniform in time bound for the original energy functional. Besides, in the error analysis, we start from the continuous in time ODE system satisfied by the error function as in [9], instead of analyzing the operator form of the numerical error function. With a careful treatment of the aliasing error and H^3 estimate of the numerical solution, we are able to derive an $\ell^\infty(0,T;\ell^2)$ error estimate for the proposed scheme.

The rest of this article is organized as follows. In Sect. 2, we present the fully discrete numerical scheme. The numerical energy stability is provided in Sect. 3, followed by $\ell^\infty(0,T;H_h^2)$ and $\ell^\infty(0,T;H_h^3)$ bounds of the numerical solution. Subsequently, an $\ell^\infty(0,T;\ell^2)$ error analysis is provided in Sect. 4, consisting of two lemmas concerning the error of the nonlinear term at any time $t\in[0,T]$ and the error of the numerical solution at $t=t_1$, respectively. In addition, numerical experiments are presented in Sect. 5, including temporal convergence test and simulation results of the scaling laws for energy, average surface roughness and average slope. Finally, some concluding remarks are given in Sect. 6.

2 Stabilized third order in time ETD multistep scheme (sETDMs3)

Some space definitions in [2] are recalled. Denote by $W^{m,p}(\Omega)$ the Sobolev space and by $\|\cdot\|_{m,p}$ the standard norm on $W^{m,p}(\Omega)$. In particular, if $p=2$, we write $W^{m,p}(\Omega)$ and $\|\cdot\|_{W^{m,2}}$ as $H^m(\Omega)$ and $\|\cdot\|_{H^m}$, respectively. Define $H^m_{\mathrm{per}}(\Omega)=\{v\in H^m(\Omega)\mid v \text{ is periodic}\}$.

Also, we follow the notations used in the Fourier pseudo-spectral method; see [5,6,13,15,25,27,32,49], etc. Let N be a positive integer, $\Omega_{\mathcal{N}}$ be a uniform $2N\times 2N$ mesh on Ω, with $(2N+1)^2$ grid points (x_i,y_j), where $x_i=ih$, $y_j=jh$ with $h:=\frac{L}{2N}$, $0\le i,j\le 2N$. Set the time step size $\tau=\frac{T}{N_t}$ and denote $t_i=i\tau$ for $0\le i\le N_t$. Define $\mathcal{M}^{\mathcal{N}}$ as the space of 2D periodic grid functions on $\Omega_{\mathcal{N}}$ and let $\mathcal{B}^N$ be the space of trigonometric polynomials in x and y of degree up to N. In this paper, we denote C one generic constant which may depend on ε, the exact solution u, the initial value u_0 and time T, but is independent of the mesh size h and time step size τ.

Now, we introduce an interpolation operator $\mathcal{I}_N$ onto $\mathcal{B}^N$ that reserves the function value on $(2N+1)^2$ grid points, i.e., $(\mathcal{I}_N g)(x_i, y_j) = g(x_i, y_j)$ for $0 \le i, j \le 2N$:

$$(\mathcal{I}_N g)(x, y) = \sum_{k,l=-N+1}^{N} (\hat{g}_c)_{k,l} \exp\left(\frac{2\pi \mathrm{i}}{L}(kx + ly)\right), \quad \text{with } \mathrm{i} = \sqrt{-1}, \tag{3}$$

where the coefficients $\{(\hat{g}_c)_{k,l}\}$ are given by the discrete Fourier transform of the $4N^2$ grid points:

$$(\hat{g}_c)_{k,l} = \frac{1}{4N^2} \sum_{i,j=1}^{2N} g(x_i, y_j) \exp\left(-\frac{2\pi \mathrm{i}}{L}(kx_i + ly_j)\right). \tag{4}$$

For any $g \in \mathcal{M}^{\mathcal{N}}$, denote $\tilde{g} = \mathcal{I}_N g$ as the continuous extension of g. When g and $\partial^\alpha g$ ($|\alpha| \le m$) are continuous and periodic on Ω, $\mathcal{I}_N$ has the following approximation property ([7, Theorem 1.2, p. 72]):

$$\|\partial^k g - \partial^k \mathcal{I}_N g\|_{\mathcal{N}} \le C \|g\|_{H_h^m} h^{m-k}, \text{ for } 0 \le k \le m,\ m > 1 \tag{5}$$

with the discrete norm and derivatives defined below.

Given $\mathcal{I}_N g$, the discrete spatial partial derivatives can be defined as:

$$(D_x g)_{i,j} = \sum_{k,l=-N+1}^{N} \frac{2k\pi \mathrm{i}}{L} (\hat{g}_c)_{k,l} \exp\left(\frac{2\pi \mathrm{i}}{L}(kx_i + ly_j)\right),$$
$$(D_x^2 g)_{i,j} = \sum_{k,l=-N+1}^{N} -\frac{4k^2\pi^2}{L^2} (\hat{g}_c)_{k,l} \exp\left(\frac{2\pi \mathrm{i}}{L}(kx_i + ly_j)\right).$$

The operators D_y and D_y^2. could be similarly defined. For any $g,\ \tilde{g} \in \mathcal{M}^{\mathcal{N}}$, and $\mathbf{g} = (g_1, g_2)^T,\ \tilde{\mathbf{g}} = (\tilde{g}_1, \tilde{g}_2)^T \in \mathcal{M}^{\mathcal{N}} \times \mathcal{M}^{\mathcal{N}}$, we introduce the discrete gradient, divergence and Laplacian operators:

$$\nabla_{\mathcal{N}} g = \begin{pmatrix} D_x g \\ D_y g \end{pmatrix}, \quad \nabla_{\mathcal{N}} \cdot g = D_x g^1 + D_y g^2, \quad \Delta_{\mathcal{N}} g = D_x^2 g + D_y^2 g.$$

Also, to measure the discrete differentiation operators defined above, we introduce the discrete L^2 (denoted as ℓ^2) inner product $(\cdot, \cdot)_{\mathcal{N}}$ and norm $\|\cdot\|_{\mathcal{N}}$:

$$(\tilde{g}, g)_{\mathcal{N}} = h^2 \sum_{i,j=1}^{2N} \tilde{g}_{ij} \bar{g}_{ij}, \qquad \|g\|_{\mathcal{N}} = \sqrt{(g, g)_{\mathcal{N}}},$$
$$(\tilde{\mathbf{g}}, \mathbf{g})_{\mathcal{N}} = h^2 \sum_{i,j=1}^{2N} (\tilde{g}_{ij}^1 \bar{g}_{ij}^1 + \tilde{g}_{ij}^2 \bar{g}_{ij}^2), \qquad \|\mathbf{g}\|_{\mathcal{N}} = \sqrt{(\mathbf{g}, \mathbf{g})_{\mathcal{N}}},$$

where $\bar{g}$ is the conjugate of g. Similarly, we can define the discrete Sobolev norm $\|\cdot\|_{H_h^2}$ and the discrete Sobolev semi-norm $|\cdot|_{H_h^2}$:

$$\|g\|_{H_h^2} = \Big(\sum_{|\alpha| \le 2} \|D^\alpha g\|_{\mathcal{N}}^2 \Big)^{\frac{1}{2}}, \quad |g|_{H_h^2} = \Big(\sum_{|\alpha| = 2} \|D^\alpha g\|_{\mathcal{N}}^2 \Big)^{\frac{1}{2}},$$

whereas above $\alpha = (\alpha_1, \alpha_2)$ is a 2-tuple of nonnegative integers with $|\alpha| = \alpha_1 + \alpha_2$, and $D^\alpha = D_x^{\alpha_1} D_y^{\alpha_2}$. Furthermore, the following summation by parts formulas are available in [32, Proposition 2.2]:

Lemma 1 *For any $\tilde{g}$, $g \in \mathcal{M}^{\mathcal{N}}$, and $\mathbf{g} = (g_1, g_2)^T \in \mathcal{M}^{\mathcal{N}} \times \mathcal{M}^{\mathcal{N}}$, we have the following summation by parts formula:*

$$(\tilde{g}, \nabla_{\mathcal{N}} \cdot \mathbf{g})_{\mathcal{N}} = -(\nabla_{\mathcal{N}} \tilde{g}, \mathbf{g})_{\mathcal{N}}, \quad (\tilde{g}, \Delta_{\mathcal{N}} g)_{\mathcal{N}} = -(\nabla_{\mathcal{N}} \tilde{g}, \nabla_{\mathcal{N}} g)_{\mathcal{N}} = (\Delta_{\mathcal{N}} \tilde{g}, g)_{\mathcal{N}}.$$

Let u_e be the exact solution to (1) and define $u := u_e \mid_{\Omega_{\mathcal{N}}}$. Also, denote $u_s^n(t_n)$ as u_s^n for $n \geq 0$. The continuous form of the sETDMs3 scheme is given by:

sETDMs3: For $n \geq 2$, find $u_s^{n+1}(t): \ [t_n, t_{n+1}] \to \mathcal{M}_0^{\mathcal{N}}$ such that

$$\frac{\mathrm{d}u_s^{n+1}(t)}{\mathrm{d}t} - A\tau^3 \frac{\mathrm{d}\Delta_{\mathcal{N}}^3 u_s^{n+1}(t)}{\mathrm{d}t} + \varepsilon^2 \Delta_{\mathcal{N}}^2 u_s^{n+1}(t) = -\sum_{i=0}^{2} \ell_i(t - t_n) f(\nabla_{\mathcal{N}} u_s^{n-i}), \tag{6}$$

where

$$\ell_0(s) = 1 + \frac{3s}{2\tau} + \frac{s^2}{2\tau^2}, \quad \ell_1(s) = -\frac{2s}{\tau} - \frac{s^2}{\tau^2}, \quad \ell_2(s) = \frac{s}{2\tau} + \frac{s^2}{2\tau^2},$$
$$\beta(\mathbf{x}) = \frac{\mathbf{x}}{1 + |\mathbf{x}|^2}, \quad f(\nabla_{\mathcal{N}} v) := \nabla_{\mathcal{N}} \cdot \beta(\nabla_{\mathcal{N}} v).$$

The regularization term has the exponent $p(3) = 3/2$ in our general framework. Higher exponents would also work at the expense of introducing higher-order error, especially for the high frequency part.

Note that we have applied the Lagrange approximation to the nonlinear term. Since the previous three steps are needed to compute the next time step, u_s^i, $k = 0, 1, 2$ are needed the initial step. Let $u_s^0 = u(0)$, as for the first step, find $u_s^1(t): \ [0, t_1] \to \mathcal{M}_0^{\mathcal{N}}$ such that

$$\frac{\mathrm{d}a_s^1(t)}{\mathrm{d}t} - A\tau^3 \frac{\mathrm{d}\Delta_{\mathcal{N}}^3 a_s^1(t)}{\mathrm{d}t} + \varepsilon^2 \Delta_{\mathcal{N}}^2 a_s^1(t) = -f(\nabla_{\mathcal{N}} u_s^0), \tag{7}$$
$$\frac{\mathrm{d}u_s^1(t)}{\mathrm{d}t} - A\tau^3 \frac{\mathrm{d}\Delta_{\mathcal{N}}^3 u_s^1(t)}{\mathrm{d}t} + \varepsilon^2 \Delta_{\mathcal{N}}^2 u_s^1(t) = -\frac{t}{\tau} f(\nabla_{\mathcal{N}} a_s^1) + \frac{t-\tau}{\tau} f(\nabla_{\mathcal{N}} u_s^0). \tag{8}$$

As for the second step, find $u_s^2(t): \ [t_1, t_2] \to \mathcal{M}_0^{\mathcal{N}}$ such that:

$$\frac{\mathrm{d}u_s^2(t)}{\mathrm{d}t} - A\tau^3 \frac{\mathrm{d}\Delta_{\mathcal{N}}^3 u_s^2(t)}{\mathrm{d}t} + \varepsilon^2 \Delta_{\mathcal{N}}^2 u_s^2(t) = -\frac{t}{\tau} f(\nabla_{\mathcal{N}} u_s^1) + \frac{t-\tau}{\tau} f(\nabla_{\mathcal{N}} u_s^0). \tag{9}$$

Note that the following consistency identity holds:

$$u_s^{k+1}(t_k) = u_s^k(t_k), \text{ for } k = 0, 1, \ldots, n. \tag{10}$$

Integrating (6)–(9) from t_n to t_{n+1}, we obtain the explicit expression of u_s^1, u_s^2 and u_s^{n+1}.

sETDMs3 (matrix form):

$$\begin{aligned}
u_s^{n+1} &= e^{-K\tau}u_s^n - \phi_0(K)\hat{f}(u_s^n)\\
&\quad - \phi_1(K)\left[\frac{3}{2}\hat{f}(u_s^n) - 2\hat{f}_{\mathcal{N}}(u_s^{n-1}) + \frac{1}{2}\hat{f}(u_s^{n-2})\right]\\
&\quad - \phi_2(K)\left[\frac{1}{2}\hat{f}(u_s^n) - \hat{f}(u_s^{n-1}) + \frac{1}{2}\hat{f}(u_s^{n-2})\right],\\
a_s^1 &= e^{-K\tau}u_s^0 - \phi_0(K)\hat{f}(u_s^0),\\
u_s^1 &= e^{-K\tau}u_s^0 - \phi_0(K)\hat{f}(u_s^0) - \phi_1(K)[\hat{f}(a_s^1) - \hat{f}(u_s^0)],\\
u_s^2 &= e^{-K\tau}u_s^1 - \phi_0(K)\hat{f}(u_s^1) - \phi_1(K)[\hat{f}(u_s^1) - \hat{f}(u_s^0)],
\end{aligned} \tag{11}$$

in which

$$\begin{aligned}
&\phi_0(K) = K^{-1}(I - e^{-K\tau}),\\
&\phi_1(K) = K^{-1}[I - (K\tau)^{-1}(I - e^{-K\tau})],\\
&\phi_2(K) = K^{-1}\{I - 2(K\tau)^{-1}[I - (K\tau)^{-1}(I - e^{-K\tau})]\},\\
&\quad K = \varepsilon^2 M^{-1}\Delta_{\mathcal{N}}^2, \qquad \hat{f}(v) = M^{-1}f(\nabla_{\mathcal{N}}v), \qquad M = I - A\tau^3\Delta_{\mathcal{N}}^3.
\end{aligned}$$

Because of the Fourier pseudo-spectral method applied in space, the sETDMs3 scheme has similar computational complexity as that of the sETDMs2 scheme in [9].

Remark 2.1 Note that the stabilization term $-A\tau^3\frac{\partial\Delta_{\mathcal{N}}^3 u(t)}{\partial t}$ can be replaced by a Dupont–Douglas type regularization term $-A\tau^2(\Delta_{\mathcal{N}}^3 u^{n+1} - \Delta_{\mathcal{N}}^3 u^n)$, similar to results in [10,14]. It is possible to construct higher-order schemes by adding a stabilization term $A(-1)^k\tau^k\frac{\partial\Delta_{\mathcal{N}}^k u(t)}{\partial t} = A\tau^k\frac{\partial(\Delta_{\mathcal{N}}^2)^{k/2}u(t)}{\partial t} = A\tau^k\frac{\partial(\Delta_{\mathcal{N}}^2)^{p(k)}u(t)}{\partial t}$ with $p(k) = k/2$, or $A(-1)^k\tau^{k-1}(\Delta_{\mathcal{N}}^k u^{n+1} - \Delta_{\mathcal{N}}^k u^n)$ if the exact solution is smooth enough. The choice of $p(k)$ is based on the consideration of (1) it is small so that the artificial error remains as small as possible, especially in the high frequency part; and (2) it is big enough so that the artificial dissipation when combined with the original dissipation term can dominate the nonlinear term which is treated explicitly. The minimal value of $p(k)$ turns out to be $k/2$ if we wish to keep the coefficient A bounded independent of ε. As for long-time computation, one way to accelerate convergence is to use various adaptive strategies, see [11,23,47,58], etc. The higher-order regularization term might introduce relatively large error for high frequency solution. Therefore, for a generic situation with random small scale initial data, it might be reasonable to take a hybrid approach similar to the blended linear response algorithm [1]: use an alternative higher-order method without regularization for the initial (phase separation) stage. The ETD-MS can be applied for the coarsening process after the elimination of very high frequency components in the solution.

3 Energy stability of sETDMs3

For simplicity, from now on we denote $\|\cdot\|_{L^2(t_i,t_j;\ell^2)}$ by $\|\cdot\|_{L^2(I_{i,j};\ell^2)}$. The following interpolation inequality is used in this section.

Lemma 2 *For any* $v \in \mathcal{M}_0^{\mathcal{N}}$,

$$\|\nabla_{\mathcal{N}}v\|_{\mathcal{N}}^2 \le \|v\|_{\mathcal{N}}^{\frac{4}{3}}\|\nabla_{\mathcal{N}}\Delta_{\mathcal{N}}v\|_{\mathcal{N}}^{\frac{2}{3}}. \tag{12}$$

Proof By Lemma 1, one can obtain

$$\|\nabla_{\mathcal{N}} v\|_{\mathcal{N}}^2 = (\nabla_{\mathcal{N}} v, \nabla_{\mathcal{N}} v)_{\mathcal{N}} = -(v, \Delta_{\mathcal{N}} v)_{\mathcal{N}} \leq \|v\|_{\mathcal{N}} \|\Delta_{\mathcal{N}} v\|_{\mathcal{N}}, \tag{13}$$

$$\|\Delta_{\mathcal{N}} v\|_{\mathcal{N}}^2 = (\Delta_{\mathcal{N}} v, \Delta_{\mathcal{N}} v)_{\mathcal{N}} = -(\nabla_{\mathcal{N}} v, \nabla_{\mathcal{N}} \Delta_{\mathcal{N}} v)_{\mathcal{N}} \leq \|\nabla_{\mathcal{N}} v\|_{\mathcal{N}} \|\nabla_{\mathcal{N}} \Delta_{\mathcal{N}} v\|_{\mathcal{N}}. \tag{14}$$

Substituting (13) into (14), one gets

$$\|\Delta_{\mathcal{N}} v\|_{\mathcal{N}} \leq \|v\|_{\mathcal{N}}^{\frac{1}{3}} \|\nabla_{\mathcal{N}} \Delta_{\mathcal{N}} v\|_{\mathcal{N}}^{\frac{2}{3}}. \tag{15}$$

A substitution of (15) into (13) completes the proof. □

Consider the following numerical energy functional:

$$\begin{aligned} &\tilde{E}(u_s^{n+1}(t)) \\ &\quad = E_{\mathcal{N}}(u_s^{n+1}(t)) + \frac{\alpha}{6}\left(\sqrt{\frac{47}{10}} + \sqrt{\frac{31}{30}}\right) \left\| \frac{\mathrm{d}u_s^{n+1}(t)}{\mathrm{d}t} \right\|_{L^2(I_{n,n+1};\ell^2)}^2 \\ &\qquad + \frac{\tau^3}{12\alpha^2}\left(\sqrt{\frac{47}{10}} + \sqrt{\frac{31}{30}}\right) \left\| \frac{\mathrm{d}\nabla_{\mathcal{N}}\Delta_{\mathcal{N}} u_s^{n+1}(t)}{\mathrm{d}t} \right\|_{L^2(I_{n,n+1};\ell^2)}^2 \\ &\qquad + \frac{\alpha}{6}\sqrt{\frac{31}{30}} \left\| \frac{\mathrm{d}u_s^{n}(t)}{\mathrm{d}t} \right\|_{L^2(I_{n-1,n};\ell^2)}^2 + \frac{\tau^3}{12\alpha^2}\sqrt{\frac{31}{30}} \left\| \frac{\mathrm{d}\nabla_{\mathcal{N}}\Delta_{\mathcal{N}} u_s^{n}(t)}{\mathrm{d}t} \right\|_{L^2(I_{n-1,n};\ell^2)}^2, \end{aligned} \tag{16}$$

where

$$E_{\mathcal{N}}(v) = \left(-\frac{1}{2}\ln(1 + |\nabla_{\mathcal{N}} v|^2), 1\right)_{\mathcal{N}} + \frac{\varepsilon^2}{2}\|\Delta_{\mathcal{N}} v\|_{\mathcal{N}}^2, \quad \forall v \in \mathcal{M}^{\mathcal{N}}, \tag{17}$$

$$\alpha = \frac{6}{9 + \sqrt{\frac{47}{10}} + \sqrt{\frac{31}{30}}}. \tag{18}$$

The main result of this section is the following theorem.

Theorem 1 *Assume that*

$$A \geq \frac{1}{2\alpha^3},$$

where $\alpha = \frac{6}{9+\sqrt{\frac{47}{10}}+\sqrt{\frac{31}{30}}}$. *Then, system* (6) *is energy stable in the sense that*

$$\tilde{E}(u_s^{n+1}) \leq \tilde{E}(u_s^n), \quad \forall n \geq 2. \tag{19}$$

Proof Taking the inner product with $\frac{\mathrm{d}u_s^{n+1}(t)}{\mathrm{d}t}$ on both sides of (6) gives that

$$\begin{aligned} &\left\| \frac{\mathrm{d}u_s^{n+1}(t)}{\mathrm{d}t} \right\|_{\mathcal{N}}^2 + A\tau^3 \left\| \frac{\mathrm{d}\nabla_{\mathcal{N}}\Delta_{\mathcal{N}} u_s^{n+1}(t)}{\mathrm{d}t} \right\|_{\mathcal{N}}^2 + \frac{\mathrm{d}}{\mathrm{d}t} E_{\mathcal{N}}(u_s^{n+1}(t)) \\ &\quad = \left(\sum_{i=0}^{2} \ell_i(t - t_n)\beta(\nabla_{\mathcal{N}} u_s^{n-i}) - \beta(\nabla_{\mathcal{N}} u_s^{n+1}(t)), \frac{\mathrm{d}\nabla_{\mathcal{N}} u_s^{n+1}(t)}{\mathrm{d}t} \right)_{\mathcal{N}}. \end{aligned} \tag{20}$$

Integrating from t_n to t_{n+1} and denoting $\beta_k = \beta(\nabla_{\mathcal{N}} u_s^k)$, one gets

$$\begin{aligned}
&\left\| \frac{\mathrm{d}u_s^{n+1}(t)}{\mathrm{d}t} \right\|^2_{L^2(I_{n,n+1};\ell^2)} + A\tau^3 \left\| \frac{\mathrm{d}\nabla_{\mathcal{N}}\Delta_{\mathcal{N}} u_s^{n+1}(t)}{\mathrm{d}t} \right\|^2_{L^2(I_{n,n+1};\ell^2)} \\
&\quad + E_{\mathcal{N}}(u_s^{n+1}) - E_{\mathcal{N}}(u_s^n) \\
&= \int_{t_n}^{t_{n+1}} \left(\beta_n - \beta(\nabla_{\mathcal{N}} u_s^{n+1}(t)), \frac{\mathrm{d}\nabla_{\mathcal{N}} u_s^{n+1}(t)}{\mathrm{d}t} \right)_{\mathcal{N}} \mathrm{d}t \\
&\quad + \int_{t_n}^{t_{n+1}} \left[\frac{3(t-t_n)}{2\tau} + \frac{(t-t_n)^2}{2\tau^2} \right] \left(\beta_n - \beta_{n-1}, \frac{\mathrm{d}\nabla_{\mathcal{N}} u_s^{n+1}(t)}{\mathrm{d}t} \right)_{\mathcal{N}} \mathrm{d}t \\
&\quad + \int_{t_n}^{t_{n+1}} \left[\frac{t-t_n}{2\tau} + \frac{(t-t_n)^2}{2\tau^2} \right] \left(\beta_{n-2} - \beta_{n-1}, \frac{\mathrm{d}\nabla_{\mathcal{N}} u_s^{n+1}(t)}{\mathrm{d}t} \right)_{\mathcal{N}} \mathrm{d}t. \qquad (21)
\end{aligned}$$

It can be easily verified that

$$\|\beta_n - \beta(\nabla_{\mathcal{N}} u_s^{n+1}(t))\|_{\mathcal{N}} \le \tau^{\frac{1}{2}} \left\| \frac{\mathrm{d}\nabla_{\mathcal{N}} u_s^{n+1}(t)}{\mathrm{d}t} \right\|_{L^2(I_{n,n+1};\ell^2)}, \qquad (22)$$

$$\|\beta_{n-k} - \beta_{n-k+1}\|_{\mathcal{N}} \le \tau^{\frac{1}{2}} \left\| \frac{\mathrm{d}\nabla_{\mathcal{N}} u_s^{n-k+1}(t)}{\mathrm{d}t} \right\|_{L^2(I_{n-k,n-k+1};\ell^2)}, \quad k = 0,\ 1. \qquad (23)$$

Substituting (22)–(23) into (21) and applying the Cauchy–Schwarz inequality, one can obtain

$$\begin{aligned}
&\text{RHS of (21)} \\
&\le \tau \left\| \frac{\mathrm{d}\nabla_{\mathcal{N}} u_s^{n+1}(t)}{\mathrm{d}t} \right\|^2_{L^2(I_{n,n+1};\ell^2)} \\
&\quad + \frac{\tau}{2}\sqrt{\frac{47}{10}} \left\| \frac{\mathrm{d}\nabla_{\mathcal{N}} u_s^{n}(t)}{\mathrm{d}t} \right\|_{L^2(I_{n-1,n};\ell^2)} \left\| \frac{\mathrm{d}\nabla_{\mathcal{N}} u_s^{n+1}(t)}{\mathrm{d}t} \right\|_{L^2(I_{n,n+1};\ell^2)} \\
&\quad + \frac{\tau}{2}\sqrt{\frac{31}{30}} \left\| \frac{\mathrm{d}\nabla_{\mathcal{N}} u_s^{n-1}(t)}{\mathrm{d}t} \right\|_{L^2(I_{n-2,n-1};\ell^2)} \left\| \frac{\mathrm{d}\nabla_{\mathcal{N}} u_s^{n+1}(t)}{\mathrm{d}t} \right\|_{L^2(I_{n,n+1};\ell^2)} \\
&\le \frac{\tau}{4}\left(4 + \sqrt{\frac{47}{10}} + \sqrt{\frac{31}{30}}\right) \left\| \frac{\mathrm{d}\nabla_{\mathcal{N}} u_s^{n+1}(t)}{\mathrm{d}t} \right\|^2_{L^2(I_{n,n+1};\ell^2)} \qquad (24) \\
&\quad + \frac{\tau}{4}\sqrt{\frac{47}{10}} \left\| \frac{\mathrm{d}\nabla_{\mathcal{N}} u_s^{n}(t)}{\mathrm{d}t} \right\|^2_{L^2(I_{n-1,n};\ell^2)} + \frac{\tau}{4}\sqrt{\frac{31}{30}} \left\| \frac{\mathrm{d}\nabla_{\mathcal{N}} u_s^{n-1}(t)}{\mathrm{d}t} \right\|^2_{L^2(I_{n-2,n-1};\ell^2)}.
\end{aligned}$$

And also, by the interpolation inequality (12), one gets

$$\begin{aligned}
\tau \left\| \frac{\mathrm{d}\nabla_{\mathcal{N}} u_s^k(t)}{\mathrm{d}t} \right\|^2_{\mathcal{N}} &\le \tau \left(\alpha^{\frac{2}{3}} \tau^{-\frac{2}{3}} \left\| \frac{\mathrm{d}u_s^k(t)}{\mathrm{d}t} \right\|^{\frac{4}{3}}_{\mathcal{N}} \right) \left(\alpha^{-\frac{2}{3}} \tau^{\frac{2}{3}} \left\| \frac{\mathrm{d}\nabla_{\mathcal{N}}\Delta_{\mathcal{N}} u_s^k(t)}{\mathrm{d}t} \right\|^{\frac{2}{3}}_{\mathcal{N}} \right) \\
&\le \frac{2\alpha}{3} \left\| \frac{\mathrm{d}u_s^k(t)}{\mathrm{d}t} \right\|^2_{\mathcal{N}} + \frac{\tau^3}{3\alpha^2} \left\| \frac{\mathrm{d}\nabla_{\mathcal{N}}\Delta_{\mathcal{N}} u_s^k(t)}{\mathrm{d}t} \right\|^2_{\mathcal{N}}, \ \forall k \ge 0. \qquad (25)
\end{aligned}$$

A substitution of (25) and (24) into (21) yields

$$\begin{aligned}
0 \geq{}& E_{\mathcal{N}}(u_s^{n+1}) + \left[1 - \left(4 + \sqrt{\frac{47}{10}} + \sqrt{\frac{31}{30}}\right)\frac{\alpha}{6}\right]\left\|\frac{\mathrm{d}u_s^{n+1}(t)}{\mathrm{d}t}\right\|^2_{L^2(I_{n,n+1};\ell^2)}\\
&+ \left[A - \left(4 + \sqrt{\frac{47}{10}} + \sqrt{\frac{31}{30}}\right)\frac{1}{12\alpha^2}\right]\tau^3\left\|\frac{\mathrm{d}\nabla_{\mathcal{N}}\Delta_{\mathcal{N}}u_s^{n+1}(t)}{\mathrm{d}t}\right\|^2_{L^2(I_{n,n+1};\ell^2)}\\
&+ \sqrt{\frac{31}{30}}\frac{\alpha}{6}\left\|\frac{\mathrm{d}u_s^{n}(t)}{\mathrm{d}t}\right\|^2_{L^2(I_{n-1,n};\ell^2)} + \sqrt{\frac{31}{30}}\frac{\tau^3}{12\alpha^2}\left\|\frac{\mathrm{d}\nabla_{\mathcal{N}}\Delta_{\mathcal{N}}u_s^{n}(t)}{\mathrm{d}t}\right\|^2_{L^2(I_{n-1,n};\ell^2)}\\
&- E_{\mathcal{N}}(u_s^{n}) - \frac{\alpha}{6}\left(\sqrt{\frac{47}{10}} + \sqrt{\frac{31}{30}}\right)\left\|\frac{\mathrm{d}u_s^{n}(t)}{\mathrm{d}t}\right\|^2_{L^2(I_{n-1,n};\ell^2)}\\
&- \frac{1}{12\alpha^2}\left(\sqrt{\frac{47}{10}} + \sqrt{\frac{31}{30}}\right)\tau^3\left\|\frac{\mathrm{d}\nabla_{\mathcal{N}}\Delta_{\mathcal{N}}u_s^{n}(t)}{\mathrm{d}t}\right\|^2_{L^2(I_{n-1,n};\ell^2)}\\
&- \sqrt{\frac{31}{30}}\frac{\alpha}{6}\left\|\frac{\mathrm{d}u_s^{n-1}(t)}{\mathrm{d}t}\right\|^2_{L^2(I_{n-2,n-1};\ell^2)}\\
&- \sqrt{\frac{31}{30}}\frac{\tau^3}{12\alpha^2}\left\|\frac{\mathrm{d}\nabla_{\mathcal{N}}\Delta_{\mathcal{N}}u_s^{n-1}(t)}{\mathrm{d}t}\right\|^2_{L^2(I_{n-2,n-1};\ell^2)}.
\end{aligned} \tag{26}$$

Since $\alpha = \frac{6}{9+\sqrt{\frac{47}{10}}+\sqrt{\frac{31}{30}}}$ and $A = \frac{1}{2\alpha^3}$, one gets

$$1 - \left(4 + \sqrt{\frac{47}{10}} + \sqrt{\frac{31}{30}}\right)\frac{\alpha}{6} > \frac{\alpha}{6}\left(\sqrt{\frac{47}{10}} + \sqrt{\frac{31}{30}}\right), \tag{27}$$

$$A - \left(4 + \sqrt{\frac{47}{10}} + \sqrt{\frac{31}{30}}\right)\frac{1}{12\alpha^2} > \frac{1}{12\alpha^2}\left(\sqrt{\frac{47}{10}} + \sqrt{\frac{31}{30}}\right). \tag{28}$$

This completes the proof of the theorem. □

A direct consequence of Theorem 1 is the following corollary.

Corollary 3.1 *Under the same assumption in Theorem 1, we have the following inequality, for any $n \geq 2$,*

$$E_{\mathcal{N}}(u_s^{n+1}) \leq \tilde{E}(u_s^{n+1}) \leq \tilde{E}(u_s^{2}). \tag{29}$$

The following estimates of $\|\nabla_{\mathcal{N}}(u^1 - a_s^1)\|_{\mathcal{N}}$ and $\|\nabla_{\mathcal{N}}(u^1 - u_s^1)\|_{\mathcal{N}}$ are needed in later analysis.

Lemma 3 *Assume that the exact solution $u_e(t)$ to (1) satisfies*

$$u_e \in H^1(I_{0,1}; H^{m+6}) \cap W^{2,\infty}(I_{0,1}; H^2).$$

Define $u(t) := u_e(t)\mid_{\Omega_{\mathcal{N}}}$ and denote $u^1 = u(t_1)$. The numerical solutions a_s^1 and u_s^1 to (7) and (8) satisfy that:

$$\|\nabla_{\mathcal{N}}(u^1 - a_s^1)\|_{\mathcal{N}} \leq C_{\varepsilon,u_e}(\tau^{\frac{1}{4}}h^m + \tau^{\frac{5}{4}}), \quad \|\nabla_{\mathcal{N}}(u^1 - u_s^1)\|_{\mathcal{N}} \leq C_{\varepsilon,u_e}(\tau^{\frac{1}{4}}h^m + \tau^{\frac{7}{4}}).$$

Proof To bound $\|\nabla_{\mathcal{N}} e_a(t_1)\|_{\mathcal{N}}$, we subtract (7) from (1) and compute the inner product with $-\Delta_{\mathcal{N}} e_a(t)$ on both sides:

$$\begin{aligned}
&\frac{1}{2}\frac{\mathrm{d}\|\nabla_{\mathcal{N}} e_a(t)\|_{\mathcal{N}}^2}{\mathrm{d}t} + \frac{A\tau^3}{2}\frac{\mathrm{d}\|\Delta_{\mathcal{N}}^2 e_a(t)\|_{\mathcal{N}}^2}{\mathrm{d}t} + \varepsilon^2\|\nabla_{\mathcal{N}}\Delta_{\mathcal{N}} e_a(t)\|_{\mathcal{N}}^2\\
&\quad = (\mathcal{R}_a(t), -\Delta_{\mathcal{N}} e_a(t))_{\mathcal{N}} \le \frac{1}{2\sqrt{\tau}}\|\Delta_{\mathcal{N}} e_a(t)\|_{\mathcal{N}}^2 + \frac{\sqrt{\tau}}{2}\|\mathcal{R}_a(t)\|_{\mathcal{N}}^2,
\end{aligned} \tag{30}$$

where $\mathcal{R}_a(t) = \sum_{i=1}^3 \mathcal{R}_i(t) + \mathcal{R}_{4,1}(t)$ and

$$\mathcal{R}_1(t) = -\varepsilon^2(\Delta^2 u_e(t)|_{\Omega_{\mathcal{N}}} - \Delta_{\mathcal{N}}^2 u(t)), \quad \mathcal{R}_2(t) = -A\tau^3\frac{\mathrm{d}\Delta_{\mathcal{N}}^3 u(t)}{\mathrm{d}t}, \tag{31}$$

$$\mathcal{R}_3(t) = \Big[\nabla_{\mathcal{N}}\cdot\beta(\nabla_{\mathcal{N}} u(t)) - \nabla\cdot\beta(\nabla u_e(t))\Big|_{\Omega_{\mathcal{N}}}\Big], \tag{32}$$

$$\mathcal{R}_{4,1}(t) = \nabla_{\mathcal{N}}\cdot\beta(\nabla_{\mathcal{N}} u^0) - \nabla_{\mathcal{N}}\cdot\beta(\nabla_{\mathcal{N}} u(t)). \tag{33}$$

Since

$$\begin{aligned}
\frac{1}{2\sqrt{\tau}}\|\Delta_{\mathcal{N}} e_a(t)\|_{\mathcal{N}}^2 &\le \frac{1}{2\sqrt{\tau}}\|\nabla_{\mathcal{N}} e_a(t)\|_{\mathcal{N}}\|\nabla_{\mathcal{N}}\Delta_{\mathcal{N}} e_a(t)\|_{\mathcal{N}}\\
&\le \frac{1}{2\tau\varepsilon^2}\|\nabla_{\mathcal{N}} e_a(t)\|_{\mathcal{N}}^2 + \frac{\varepsilon^2}{2}\|\nabla_{\mathcal{N}}\Delta_{\mathcal{N}} e_a(t)\|_{\mathcal{N}}^2,
\end{aligned} \tag{34}$$

we define $\phi_a(t) = \frac{1}{2}\|\nabla_{\mathcal{N}} e_a(t)\|_{\mathcal{N}}^2 + \frac{A\tau^3}{2}\|\Delta_{\mathcal{N}}^2 e_a(t)\|_{\mathcal{N}}^2$ and get

$$\frac{\mathrm{d}\phi_a(t)}{\mathrm{d}t} \le \frac{1}{\tau\varepsilon^2}\phi_a(t) + \frac{\sqrt{\tau}}{2}\|\mathcal{R}_a(t)\|_{\mathcal{N}}^2. \tag{35}$$

Integrating (35) from 0 to t_1 and recalling that $e_a(0) = 0$, one obtains

$$\|\nabla_{\mathcal{N}} e_a(t_1)\|_{\mathcal{N}}^2 \le \sqrt{\tau}e^{1/\varepsilon^2}\|\mathcal{R}_a(t)\|_{L^2(I_{0,1};\ell^2)}^2. \tag{36}$$

Note that $\mathcal{R}_i(t) = \widetilde{\mathcal{R}}_i(t)\Big|_{\Omega_{\mathcal{N}}}$ for $1 \le i \le 3$, with

$$\|\widetilde{\mathcal{R}}_1(t)\|_{L^2} = \|-\varepsilon^2\left(\Delta^2 u_e(t) - \Delta^2\mathcal{I}_N u(t)\right)\|_{L^2} \le C\varepsilon^2 h^m\|u_e(t)\|_{H^{m+4}}, \tag{37}$$

$$\begin{aligned}
\|\widetilde{\mathcal{R}}_2(t)\|_{L^2} &= \left\|A\tau^3\frac{\mathrm{d}\Delta^3\mathcal{I}_N u_e(t)}{\mathrm{d}t}\right\|_{L^2} = A\tau^3\left\|\Delta^3\mathcal{I}_N\frac{\mathrm{d}u_e(t)}{\mathrm{d}t}\right\|_{L^2}\\
&\le C\tau^3 h^m\left\|\frac{\mathrm{d}u_e(t)}{\mathrm{d}t}\right\|_{H^{m+6}} + A\tau^3\left\|\frac{\mathrm{d}u_e(t)}{\mathrm{d}t}\right\|_{H^6},
\end{aligned} \tag{38}$$

$$\begin{aligned}
\|\widetilde{\mathcal{R}}_3(t)\|_{L^2} &= \|\nabla\cdot[\beta(\nabla\mathcal{I}_N u_e(t)) - \beta(\nabla u_e(t))]\|_{L^2} \le C\|\mathcal{I}_N u_e(t) - u_e(t)\|_{H^2}\\
&\le C\|u_e(t)\|_{H^{m+2}}h^m,
\end{aligned} \tag{39}$$

where we have applied the approximation property of $\mathcal{I}_N$ in (5). Combining with the estimate for $\mathcal{R}_{4,1}(t)$ in (33), one arrives at

$$\|\mathcal{R}_a(t)\|_{L^2(I_{0,1};\ell^2)}^2 \le C(h^{2m} + \tau^2)\left[\|u_e(t)\|_{H^1(I_{0,1};H^{m+6})}^2 + \|u_e(t)\|_{W^{1,\infty}(I_{0,1};H^2)}^2\right]. \tag{40}$$

A substitution of (40) into (36) leads to

$$\|\nabla_{\mathcal{N}} e_a(t_1)\|_{\mathcal{N}}^2 \le C_{\varepsilon,u_e}(\tau^{\frac{1}{2}}h^{2m} + \tau^{\frac{5}{2}}). \tag{41}$$

To estimate $\|\nabla_{\mathcal{N}} e(t_1)\|_{\mathcal{N}}$, by subtracting (8) from (1) and computing the inner product with $-\Delta_{\mathcal{N}} e(t)$, one gets

$$\begin{aligned}
&\frac{1}{2}\frac{\mathrm{d}\|\nabla_{\mathcal{N}} e(t)\|_{\mathcal{N}}^2}{\mathrm{d}t} + \frac{A\tau^3}{2}\frac{\mathrm{d}\|\Delta_{\mathcal{N}}^2 e(t)\|_{\mathcal{N}}^2}{\mathrm{d}t} + \varepsilon^2\|\nabla_{\mathcal{N}}\Delta_{\mathcal{N}} e(t)\|_{\mathcal{N}}^2 \\
&\quad = \left(\mathcal{R}_{u_s^1}(t), -\Delta_{\mathcal{N}} e(t)\right)_{\mathcal{N}} - \frac{t}{\tau}\left(\beta(\nabla_{\mathcal{N}} u^1) - \beta(\nabla_{\mathcal{N}} a_s^1), \nabla_{\mathcal{N}}\Delta_{\mathcal{N}} e(t)\right)_{\mathcal{N}} \\
&\quad \le \frac{1}{2\tau\varepsilon^2}\|\nabla_{\mathcal{N}} e(t)\|_{\mathcal{N}}^2 + \frac{\varepsilon^2}{2}\|\nabla_{\mathcal{N}}\Delta_{\mathcal{N}} e(t)\|_{\mathcal{N}}^2 + \frac{\sqrt{\tau}}{2}\|\mathcal{R}_{u_s^1}(t)\|_{\mathcal{N}}^2 \\
&\qquad + \frac{C_{\varepsilon,u_e}}{2\varepsilon^2}(\tau^{\frac{1}{2}}h^{2m} + \tau^{\frac{5}{2}}) + \frac{\varepsilon^2}{2}\|\nabla_{\mathcal{N}}\Delta_{\mathcal{N}} e(t)\|_{\mathcal{N}}^2,
\end{aligned} \tag{42}$$

where (41) and the Cauchy–Schwarz inequality have been applied. Besides, we have $\mathcal{R}_{u_s^1}(t) := \sum_{i=1}^3 \mathcal{R}_i(t) + \mathcal{R}_{4,2}(t)$, in which

$$\begin{aligned}
\mathcal{R}_{4,2}(t) &= \frac{t}{\tau}\nabla_{\mathcal{N}}\cdot\beta(\nabla_{\mathcal{N}} u^1) - \frac{t-\tau}{\tau}\nabla_{\mathcal{N}}\cdot\beta(\nabla_{\mathcal{N}} u^0) - \nabla_{\mathcal{N}}\cdot\beta(\nabla_{\mathcal{N}} u(t)) \\
&= \int_t^\tau \frac{t(\tau-s)}{\tau}\partial_{tt} f(\nabla_{\mathcal{N}} u(s))\,\mathrm{d}s + \int_t^0 \frac{s(t-\tau)}{\tau}\partial_{tt} f(\nabla_{\mathcal{N}} u(s))\,\mathrm{d}s,
\end{aligned} \tag{43}$$

satisfying that

$$\|\mathcal{R}_{4,2}(t)\|_{L^2(I_{0,1};\ell^2)}^2 \le \tau\|\mathcal{R}_{4,2}(t)\|_{L^\infty(I_{0,1};\ell^2)}^2 \le C\tau^5\|f(\nabla_{\mathcal{N}} u(t))\|_{W^{2,\infty}(I_{0,1};\ell^2)}^2. \tag{44}$$

Note that $e(0) = 0$. Repeating the analyses as in (35)–(36), one gets

$$\begin{aligned}
\|\nabla_{\mathcal{N}} e(t_1)\|_{\mathcal{N}}^2 &\le 2e^{1/\varepsilon^2}\left(\frac{\sqrt{\tau}}{2}\|\mathcal{R}_{u_s^1}(t)\|_{L^2(I_{0,1};\ell^2)}^2 + C_{\varepsilon,u_e}(\tau^{\frac{3}{2}}h^{2m} + \tau^{\frac{7}{2}})\right) \\
&\le C_{\varepsilon,u_e}(\tau^{\frac{7}{2}} + \tau^{\frac{1}{2}}h^{2m}).
\end{aligned} \tag{45}$$

This completes the proof. □

Given above energy stability and the fact that $u_s^{n+1}(t) \in \mathcal{M}_0^{\mathcal{N}}$, we can derive a uniform in time bound of $\|u_s^{n+1}(t)\|_{H_h^2}^2$.

Lemma 4 *Assume that $A \ge \frac{1}{2\alpha^3}$, and the exact solution u_e satisfies*

$$u_e \in H^1(I_{0,1}; H^{m+6}) \cap W^{2,\infty}(I_{0,1}; H^2).$$

Then, one has a global in time bound for solutions of (6): for $0 \le n \le N_t - 1$,

$$E_{\mathcal{N}}(u_s^{n+1}) \le E_{\mathcal{N}}(u_s^0) + C_{\varepsilon,u_e}(\tau^{\frac{5}{2}} + \tau^{\frac{1}{2}}h^{2m}), \quad \|u_s^{n+1}(t)\|_{H_h^2}^2 \le C_1,$$

where C_1 only depends on ε, X, u_0 and u_e.

Proof Taking the inner product with $\frac{\mathrm{d}u_s^2(t)}{\mathrm{d}t}$ on both sides of (9), and repeating the analyses as in (21)–(26), we get

$$\begin{aligned}
&\left\|\frac{\mathrm{d}u_s^2(t)}{\mathrm{d}t}\right\|^2_{L^2(I_{1,2};\ell^2)} + A\tau^3\left\|\frac{\mathrm{d}\nabla_{\mathcal{N}}\Delta_{\mathcal{N}}u_s^2(t)}{\mathrm{d}t}\right\|^2_{L^2(I_{1,2};\ell^2)} + E_{\mathcal{N}}(u_s^2) - E_{\mathcal{N}}(u_s^1)\\
&\quad\le \frac{5\alpha}{6}\left\|\frac{\mathrm{d}u_s^2(t)}{\mathrm{d}t}\right\|^2_{L^2(I_{1,2};\ell^2)} + \frac{5\tau^3}{12\alpha^2}\left\|\frac{\mathrm{d}\nabla_{\mathcal{N}}\Delta_{\mathcal{N}}u_s^2(t)}{\mathrm{d}t}\right\|^2_{L^2(I_{1,2};\ell^2)}\\
&\qquad+\frac{\alpha}{6}\left\|\frac{\mathrm{d}u_s^1(t)}{\mathrm{d}t}\right\|^2_{L^2(I_{0,1};\ell^2)} + \frac{\tau^3}{12\alpha^2}\left\|\frac{\mathrm{d}\nabla_{\mathcal{N}}\Delta_{\mathcal{N}}u_s^1(t)}{\mathrm{d}t}\right\|^2_{L^2(I_{0,1};\ell^2)}\\
&\quad\le\left(4+\sqrt{\frac{47}{10}}\right)\frac{\alpha}{6}\left\|\frac{\mathrm{d}u_s^2(t)}{\mathrm{d}t}\right\|^2_{L^2(I_{1,2};\ell^2)}\\
&\qquad+\left(4+\sqrt{\frac{47}{10}}\right)\frac{\tau^3}{12\alpha^2}\left\|\frac{\mathrm{d}\nabla_{\mathcal{N}}\Delta_{\mathcal{N}}u_s^2(t)}{\mathrm{d}t}\right\|^2_{L^2(I_{1,2};\ell^2)}\\
&\qquad+\sqrt{\frac{47}{10}}\frac{\alpha}{6}\left\|\frac{\mathrm{d}u_s^1(t)}{\mathrm{d}t}\right\|^2_{L^2(I_{0,1};\ell^2)} + \sqrt{\frac{47}{10}}\frac{\tau^3}{12\alpha^2}\left\|\frac{\mathrm{d}\nabla_{\mathcal{N}}\Delta_{\mathcal{N}}u_s^1(t)}{\mathrm{d}t}\right\|^2_{L^2(I_{0,1};\ell^2)},
\end{aligned}\tag{46}$$

where $\alpha = \frac{6}{9+\sqrt{\frac{47}{10}}+\sqrt{\frac{31}{30}}}$ is defined as above. Rearranging terms, one obtains

$$\begin{aligned}
\tilde{E}(u_s^2) \le E_{\mathcal{N}}(u_s^1) &+ \left(\sqrt{\frac{47}{10}}+\sqrt{\frac{31}{30}}\right)\frac{\alpha}{6}\left\|\frac{\mathrm{d}u_s^1(t)}{\mathrm{d}t}\right\|^2_{L^2(I_{0,1};\ell^2)}\\
&+\left(\sqrt{\frac{47}{10}}+\sqrt{\frac{31}{30}}\right)\frac{\tau^3}{12\alpha^2}\left\|\frac{\mathrm{d}\nabla_{\mathcal{N}}\Delta_{\mathcal{N}}u_s^1(t)}{\mathrm{d}t}\right\|^2_{L^2(I_{0,1};\ell^2)}.
\end{aligned}\tag{47}$$

On the other hand, taking the inner product with $\frac{\mathrm{d}u_s^1(t)}{\mathrm{d}t}$ on both sides of the equation satisfied by $u_s^1(t)$ and repeating the analyses as in (21)–(24), we also have

$$\begin{aligned}
&\left\|\frac{\mathrm{d}u_s^1(t)}{\mathrm{d}t}\right\|^2_{L^2(I_{0,1};\ell^2)} + A\tau^3\left\|\frac{\mathrm{d}\nabla_{\mathcal{N}}\Delta_{\mathcal{N}}u_s^1(t)}{\mathrm{d}t}\right\|^2_{L^2(I_{0,1};\ell^2)} + E_{\mathcal{N}}(u_s^1) - E_{\mathcal{N}}(u_s^0)\\
&\quad\le \|\nabla_{\mathcal{N}}(a_s^1-u_s^1(t))\|_{L^2(I_{0,1};\ell^2)}\left\|\frac{\mathrm{d}\nabla_{\mathcal{N}}u_s^1(t)}{\mathrm{d}t}\right\|_{L^2(I_{0,1};\ell^2)} + \tau\left\|\frac{\mathrm{d}\nabla_{\mathcal{N}}u_s^1(t)}{\mathrm{d}t}\right\|^2_{L^2(I_{0,1};\ell^2)}.
\end{aligned}\tag{48}$$

Splitting $\|\nabla_{\mathcal{N}}(a_s^1-u_s^1(t))\|_{L^2(I_{0,1};\ell^2)}$ into three parts, combined with an application of Lemma 3 and the Cauchy–Schwarz inequality, we arrive at

$$\begin{aligned}
&\|\nabla_{\mathcal{N}}(a_s^1-u_s^1(t))\|_{L^2(I_{0,1};\ell^2)}\left\|\frac{\mathrm{d}\nabla_{\mathcal{N}}u_s^1(t)}{\mathrm{d}t}\right\|_{L^2(I_{0,1};\ell^2)}\\
&\quad\le\sqrt{\tau}\left(\|\nabla_{\mathcal{N}}(a_s^1-u^1)\|_{\mathcal{N}}+\|\nabla_{\mathcal{N}}(u^1-u_s^1)\|_{\mathcal{N}}\right)\left\|\frac{\mathrm{d}\nabla_{\mathcal{N}}u_s^1(t)}{\mathrm{d}t}\right\|_{L^2(I_{0,1};\ell^2)}\\
&\qquad+\|\nabla_{\mathcal{N}}(u_s^1-u_s^1(t))\|_{L^2(I_{0,1};\ell^2)}\left\|\frac{\mathrm{d}\nabla_{\mathcal{N}}u_s^1(t)}{\mathrm{d}t}\right\|_{L^2(I_{0,1};\ell^2)}\\
&\quad\le C_{\varepsilon,u_e}(\tau^{\frac{5}{2}}+\tau^{\frac{1}{2}}h^{2m})+\frac{5\tau}{4}\left\|\frac{\mathrm{d}\nabla_{\mathcal{N}}u_s^1(t)}{\mathrm{d}t}\right\|^2_{L^2(I_{0,1};\ell^2)}.
\end{aligned}\tag{49}$$

Substituting (49) into (48), applying (12), one gets

$$\begin{aligned} &E_{\mathcal{N}}(u_s^0) + C_{\varepsilon,u_e}(\tau^{\frac{5}{2}} + \tau^{\frac{1}{2}} h^{2m}) \\ &\quad \geq E_{\mathcal{N}}(u_s^1) + \left(1 - \frac{9}{4} \cdot \frac{2\alpha}{3}\right) \left\| \frac{\mathrm{d}u_s^1(t)}{\mathrm{d}t} \right\|^2_{L^2(I_{0,1};\ell^2)} \\ &\qquad + \left(A - \frac{9}{4} \cdot \frac{1}{3\alpha^2}\right) \tau^3 \left\| \frac{\mathrm{d}\nabla_{\mathcal{N}} \Delta_{\mathcal{N}} u_s^1(t)}{\mathrm{d}t} \right\|^2_{L^2(I_{0,1};\ell^2)}. \end{aligned} \tag{50}$$

Meanwhile, it can be verified that

$$1 - \frac{9}{4} \cdot \frac{2\alpha}{3} = \left(\sqrt{\frac{47}{10}} + \sqrt{\frac{31}{30}}\right) \frac{\alpha}{6}, \quad A - \frac{9}{4} \cdot \frac{1}{3\alpha^2} = \left(\sqrt{\frac{47}{10}} + \sqrt{\frac{31}{30}}\right) \frac{1}{12\alpha^2}.$$

Therefore, a combination of (47), (50) and Corollary 3.1 leads to

$$E_{\mathcal{N}}(u_s^{n+1}) \leq E_{\mathcal{N}}(u_s^0) + C_{\varepsilon,u_e}(\tau^{\frac{5}{2}} + \tau^{\frac{1}{2}} h^{2m}). \tag{51}$$

Finally, applying Lemma 3.2 and Remark 3.3 in [10, p. 586], we complete the proof. □

Next, we provide a finite time H_h^3 bound for the numerical solution $u_s^{n+1}(t)$, which shall be used in the convergence analysis.

Lemma 5 *Assume that the initial solution $u(0)$ has H_h^6-regularity and A satisfies the requirement in Theorem 1. Then, we have the finite time H_h^3 bound for the numerical solution*

$$\|u_s^{n+1}(t)\|^2_{H_h^3} \leq C_1, \quad \textit{for } 0 \leq n \leq N_t - 1, \tag{52}$$

where C_1 only depends on ε, Ω and $\|u(0)\|_{H_h^6}$.

Proof Taking an inner product with $-\Delta_{\mathcal{N}}^3 u_s^{n+1}(t)$ on both sides of (6) leads to

$$\begin{aligned} &\frac{1}{2} \frac{\mathrm{d}\|\nabla_{\mathcal{N}} \Delta_{\mathcal{N}} u_s^{n+1}(t)\|^2_{\mathcal{N}}}{\mathrm{d}t} + \frac{A\tau^3}{2} \frac{\mathrm{d}\|\Delta_{\mathcal{N}}^3 u_s^{n+1}(t)\|^2_{\mathcal{N}}}{\mathrm{d}t} + \varepsilon^2 \|\nabla_{\mathcal{N}} \Delta_{\mathcal{N}}^2 u_s^{n+1}(t)\|^2_{\mathcal{N}} \\ &\quad = \sum_{i=0}^{2} \ell_i(t - t_n) \Big(\nabla_{\mathcal{N}} \nabla_{\mathcal{N}} \cdot \beta(\nabla_{\mathcal{N}} u_s^n), \nabla_{\mathcal{N}} \Delta_{\mathcal{N}}^2 u_s^{n+1}(t)\Big)_{\mathcal{N}}. \end{aligned} \tag{53}$$

For any $v \in H_h^2(\Omega)$ with periodic boundary conditions, recall that $\tilde{v} = \mathcal{I}_N v$ is the continuous extension of v. As in [9, Proposition 3.4], by using (5), for $\tilde{v} = \tilde{u}_s^n,\ \tilde{u}_s^{n-1},\ \tilde{u}_s^{n-2}$, one has

$$\|\nabla_{\mathcal{N}} \nabla_{\mathcal{N}} \cdot \beta(v)\|_{\mathcal{N}} = \|\nabla\nabla \cdot \mathcal{I}_N(\beta(\nabla\tilde{v}))\| \leq C\|\beta(\nabla\tilde{v})\|_{H^2} \leq C\|\nabla\Delta\tilde{v}\|, \tag{54}$$

in which we have used the H^2 bound of $\tilde{v}$. Substituting the above estimates into (53) and applying Lemma 4, one gets

$$\begin{aligned} &\frac{1}{2} \frac{\mathrm{d}\|\nabla_{\mathcal{N}} \Delta_{\mathcal{N}} u_s^{n+1}(t)\|^2_{\mathcal{N}}}{\mathrm{d}t} + \frac{A\tau^3}{2} \frac{\mathrm{d}\|\Delta_{\mathcal{N}}^3 u_s^{n+1}(t)\|^2_{\mathcal{N}}}{\mathrm{d}t} + \varepsilon^2 \|\nabla_{\mathcal{N}} \Delta_{\mathcal{N}}^2 u_s^{n+1}(t)\|^2_{\mathcal{N}} \\ &\quad \leq \frac{\varepsilon^2}{2} \|\nabla_{\mathcal{N}} \Delta_{\mathcal{N}}^2 u_s^{n+1}(t)\|^2_{\mathcal{N}} + C\varepsilon^{-2} \sum_{k=0}^{2} \|\nabla_{\mathcal{N}} \Delta_{\mathcal{N}} u_s^{n-k}\|^2_{\mathcal{N}}. \end{aligned} \tag{55}$$

In turn, an integration from t_n to t_{n+1} implies that

$$\frac{1}{2}\left(\|\nabla_{\mathcal{N}}\Delta_{\mathcal{N}}u_s^{n+1}\|_{\mathcal{N}}^2-\|\nabla_{\mathcal{N}}\Delta_{\mathcal{N}}u_s^{n}\|_{\mathcal{N}}^2\right)+\frac{A\tau^3}{2}\left(\|\Delta_{\mathcal{N}}^3u_s^{n+1}\|_{\mathcal{N}}^2-\|\Delta_{\mathcal{N}}^3u_s^{n}\|_{\mathcal{N}}^2\right)$$
$$\le C\varepsilon^{-2}\tau\sum_{k=0}^{2}\|\nabla_{\mathcal{N}}\Delta_{\mathcal{N}}u_s^{n-k}\|_{\mathcal{N}}^2. \tag{56}$$

Note that for $n=0$ and 1 the same expression as (56) can be obtained, except that the summation part on the RHS only contains two terms. In particular, when $n=0$, the $\|\nabla_{\mathcal{N}}\Delta_{\mathcal{N}}a_s^1\|_{\mathcal{N}}^2$ term is on the RHS. To analyze this term, repeating the process in (53)–(56) on (7), we get

$$\|\nabla_{\mathcal{N}}\Delta_{\mathcal{N}}a_s^1\|_{\mathcal{N}}^2\le(1+C\varepsilon^{-2}\tau)\|\nabla_{\mathcal{N}}\Delta_{\mathcal{N}}u_s^0\|_{\mathcal{N}}^2+A\tau^3\|\Delta_{\mathcal{N}}^3u_s^0\|_{\mathcal{N}}^2. \tag{57}$$

Now, a summation of (56) from 0 to n shows that

$$\frac{1}{2}\|\nabla_{\mathcal{N}}\Delta_{\mathcal{N}}u_s^{n+1}\|_{\mathcal{N}}^2+\frac{A\tau^3}{2}\|\Delta_{\mathcal{N}}^3u_s^{n+1}\|_{\mathcal{N}}^2$$
$$\le C\tau\varepsilon^{-2}\sum_{i=0}^{n}\|\nabla_{\mathcal{N}}\Delta_{\mathcal{N}}u_s^{i}\|_{\mathcal{N}}^2+\|\nabla_{\mathcal{N}}\Delta_{\mathcal{N}}u_s^0\|_{\mathcal{N}}^2+A\tau^3\|\Delta_{\mathcal{N}}^3u_s^0\|_{\mathcal{N}}^2.$$

An application of the discrete Gronwall's inequality leads to

$$\|\nabla_{\mathcal{N}}\Delta_{\mathcal{N}}u_s^{n+1}\|_{\mathcal{N}}\le C, \tag{58}$$

where C depends only on $\varepsilon,\ u(0)$ and T. □

4 Error analysis of the sETDMs3 scheme

Here, we recall a modified version of Lemma 4.3 in [9]:

Lemma 6 *For any $v,\ w,\ \mathcal{M}_0^{\mathcal{N}}\cap H_h^3$ and $g\in\mathcal{M}^{\mathcal{N}}\cap H_h^2$, we have*

$$\left(\beta(\nabla_{\mathcal{N}}v)-\beta(\nabla_{\mathcal{N}}w),\nabla_{\mathcal{N}}g\right)_{\mathcal{N}}$$
$$\le C_{v,w}(1+h)\left(\frac{1}{4\lambda_1\varepsilon^2}+\frac{1}{4\lambda_2}\right)\|v-w\|_{\mathcal{N}}^2+\lambda_1\varepsilon^2\|\Delta_{\mathcal{N}}g\|_{\mathcal{N}}^2+\lambda_2\|g\|_{\mathcal{N}}^2,$$

where $C_{v,w}$ is a constant depending on Ω, $\|w\|_{H_h^3}$ and $\|v\|_{H_h^3}$, λ_1 and λ_2 are any positive constants.

Proof With Lemma 5, the proof is almost the same as in [9, Lemma 4.3], except that the parameters in the Cauchy–Schwarz inequalities in the last step are chosen as λ_1 and λ_2. □

The following estimate for the initial step error is needed in the later analysis.

Lemma 7 *Assume that A satisfies the assumptions in Lemma 5, $u(0)$ has H_h^{11}-regularity, and the exact solution u_e to (1) satisfies the regularity*

$$u_e\in H^1(0,T;H_{per}^{m+7}(\Omega))\cap H^2(0,T;H_{per}^3(\Omega)).$$

Then, one obtains

$$\frac{1}{2}\|u(t_1)-u_s^1\|_{\mathcal{N}}^2+\frac{A\tau^3}{2}\|\nabla_{\mathcal{N}}\Delta_{\mathcal{N}}(u(t_1)-u_s^1)\|_{\mathcal{N}}^2\le C(h^{2m}+\tau^6). \tag{59}$$

Proof Recall that $f(\nabla_{\mathcal{N}}v)=\nabla_{\mathcal{N}}\cdot\beta(\nabla_{\mathcal{N}}v)$. An application of Taylor expansion indicates that

$$f(\nabla_{\mathcal{N}}a_s^1)=f(\nabla_{\mathcal{N}}u_s^0)+\tau\frac{\mathrm{d}f(\nabla_{\mathcal{N}}u_s^0)}{\mathrm{d}t}+\int_0^\tau\frac{\mathrm{d}^2f(\nabla_{\mathcal{N}}a_s^1(l))}{\mathrm{d}l^2}(\tau-l)\mathrm{d}l, \tag{60}$$

$$f(\nabla_{\mathcal{N}}u(t))=f(\nabla_{\mathcal{N}}u_s^0)+t\frac{\mathrm{d}f(\nabla_{\mathcal{N}}u(0))}{\mathrm{d}t}+\int_0^t\frac{\mathrm{d}^2f(\nabla_{\mathcal{N}}u(l))}{\mathrm{d}l^2}(t-l)\mathrm{d}l, \tag{61}$$

in which

$$\frac{\mathrm{d}f(\nabla_{\mathcal{N}}v)}{\mathrm{d}t}=\nabla_{\mathcal{N}}\cdot\left(\frac{\nabla_{\mathcal{N}}v_t}{1+|\nabla_{\mathcal{N}}v|^2}\right)-2\nabla_{\mathcal{N}}\cdot\left(\frac{|\nabla_{\mathcal{N}}v_t||\nabla_{\mathcal{N}}v|\nabla_{\mathcal{N}}v}{1+|\nabla_{\mathcal{N}}v|^2}\right). \tag{62}$$

Recall that $M=I-A\tau^3\Delta_{\mathcal{N}}^3$, $K=\varepsilon^2M^{-1}\Delta_{\mathcal{N}}^2$. By (7) and (1), one gets

$$\frac{\mathrm{d}u_s^0}{\mathrm{d}t}=M^{-1}\left[-KMu_s^0-f(u_s^0)\right], \tag{63}$$

$$\frac{\mathrm{d}u(0)}{\mathrm{d}t}=M^{-1}\left[-KMu_s^0-f(u_s^0)+\sum_{i=1}^3\mathcal{R}_i(0)\right], \tag{64}$$

where $\sum_{i=1}^3\mathcal{R}_i(0)$ are defined as in (31)–(32). A substitution of (60)–(64) into (7) gives

$$\frac{\mathrm{d}u_s^1(t)}{\mathrm{d}t}+A\tau^3\frac{\mathrm{d}\Delta_{\mathcal{N}}^3u_s^1(t)}{\mathrm{d}t}+\varepsilon^2\Delta_{\mathcal{N}}^2u_s^1(t)=-f(u(t))+\sum_{i=1}^3\hat{R}_i(t), \tag{65}$$

with

$$\hat{R}_1(t)=t\left(\frac{\mathrm{d}f(\nabla_{\mathcal{N}}u(0))}{\mathrm{d}t}-\frac{\mathrm{d}f(\nabla_{\mathcal{N}}u_s^0)}{\mathrm{d}t}\right), \tag{66}$$

$$\hat{R}_2(t)=\int_0^t\frac{\mathrm{d}^2f(\nabla_{\mathcal{N}}u(l))}{\mathrm{d}l^2}(t-l)\,\mathrm{d}l, \tag{67}$$

$$\hat{R}_3(t)=-\frac{t}{\tau}\int_0^\tau\frac{\mathrm{d}^2f(\nabla_{\mathcal{N}}a_s^1(l))}{\mathrm{d}l^2}(\tau-l)\mathrm{d}l. \tag{68}$$

Define the error function as $e(t)=u(t)-u_s^1(t)$, then one gets

$$\frac{\mathrm{d}e(t)}{\mathrm{d}t}+A\tau^3\frac{\mathrm{d}\Delta_{\mathcal{N}}^3e(t)}{\mathrm{d}t}+\varepsilon^2\Delta_{\mathcal{N}}^2e(t)=-\sum_{i=1}^3\hat{R}_i(t)+\sum_{i=1}^3\mathcal{R}_i(t). \tag{69}$$

Taking the inner product with $e(t)$ on both sides, and denoting

$$\omega(t):=\frac{1}{2}\|e(t)\|_{\mathcal{N}}^2+\frac{A\tau^3}{2}\|\nabla_{\mathcal{N}}\Delta_{\mathcal{N}}e(t)\|_{\mathcal{N}}^2, \tag{70}$$

one gets

$$\frac{\mathrm{d}\omega(t)}{\mathrm{d}t}+\varepsilon^2\|\Delta_{\mathcal{N}}e(t)\|_{\mathcal{N}}^2\le\frac{\|e(t)\|_{\mathcal{N}}^2}{4\tau}+3\tau\sum_{i=1}^{3}\|\mathcal{R}_i(t)\|_{\mathcal{N}}^2+\sum_{i=1}^{3}\left(\hat{R}_i(t),e(t)\right)_{\mathcal{N}}. \tag{71}$$

For $\left(\hat{R}_1(t),e(t)\right)_{\mathcal{N}}$, using integration by parts, the Cauchy–Schwarz inequality, and $u(0)=u_s^0$, one has

$$\begin{aligned}
&\left(\hat{R}_1(t),e(t)\right)_{\mathcal{N}}\\
&=-\left(\frac{\nabla_{\mathcal{N}}\left(\frac{\mathrm{d}u_s^0}{\mathrm{d}t}-\frac{\mathrm{d}u_s^0}{\mathrm{d}t}\right)}{1+|\nabla_{\mathcal{N}}u_s^0|^2},\nabla_{\mathcal{N}}e(t)\right)_{\mathcal{N}}\\
&\quad+2\left(\frac{\left(\left|\nabla_{\mathcal{N}}\frac{\mathrm{d}u(0)}{\mathrm{d}t}\right|-\left|\nabla_{\mathcal{N}}\frac{\mathrm{d}u_s^0}{\mathrm{d}t}\right|\right)|\nabla_{\mathcal{N}}u_s^0|\nabla_{\mathcal{N}}u_s^0}{1+|\nabla_{\mathcal{N}}u_s^0|^2},\nabla_{\mathcal{N}}e(t)\right)_{\mathcal{N}}\\
&\le 3\|\nabla_{\mathcal{N}}e(t)\|_{\mathcal{N}}\sum_{i=1}^{3}\|\nabla_{\mathcal{N}}\mathcal{R}_i(0)\|_{\mathcal{N}}\\
&\le 3(\|e(t)\|_{\mathcal{N}}+\|\Delta_{\mathcal{N}}e(t)\|_{\mathcal{N}})\sum_{i=1}^{3}\|\nabla_{\mathcal{N}}\mathcal{R}_i(0)\|_{\mathcal{N}}\\
&\le\frac{1}{4\tau}\|e(t)\|_{\mathcal{N}}^2+\frac{\varepsilon^2}{2}\|\Delta_{\mathcal{N}}e(t)\|_{\mathcal{N}}^2+\left(\frac{27}{2\varepsilon^2}+27\tau\right)\sum_{i=1}^{3}\|\nabla_{\mathcal{N}}\mathcal{R}_i(0)\|_{\mathcal{N}}^2.
\end{aligned}\tag{72}$$

Next, $\left(\hat{R}_i(t),e(t)\right)_{\mathcal{N}}$ with $i=2,3$ can be analyzed using (44):

$$\begin{aligned}
&\sum_{i=2}^{3}\left(\hat{R}_i(t),e(t)\right)_{\mathcal{N}}\\
&\le\tau^{\frac{3}{2}}\|e(t)\|_{\mathcal{N}}\left(\left\|\frac{\mathrm{d}^2f(\nabla_{\mathcal{N}}u(t))}{\mathrm{d}t^2}\right\|_{L^2(I_{0,1};\ell^2)}+\left\|\frac{\mathrm{d}^2f(\nabla_{\mathcal{N}}a_s^1(t))}{\mathrm{d}t^2}\right\|_{L^2(I_{0,1};\ell^2)}\right)\\
&\le\frac{1}{4\tau}\|e(t)\|_{\mathcal{N}}^2+\tau^5\left\|f(\nabla_{\mathcal{N}}u(t))\right\|_{W^{2,\infty}(I_{0,1};\ell^2)}^2+\tau^5\left\|f(\nabla_{\mathcal{N}}a_s^1(t))\right\|_{W^{2,\infty}(I_{0,1};\ell^2)}^2\\
&\le\frac{1}{4\tau}\|e(t)\|_{\mathcal{N}}^2+C\tau^5(\|u(t)\|_{H^2(I_{0,1};H_h^3)}^2+\|a_s^1(t)\|_{H^2(I_{0,1};H_h^3)}^2),
\end{aligned}\tag{73}$$

where the regularity of $a_s^1(t)$ is obtained by its closed form in (11), the assumption that $u(0)$ has H_h^{11}-regularity:

$$\begin{aligned}
\|a_s^1(t)\|_{H^2(I_{0,1};H_h^3)}^2&\le C\tau\left\|\Delta_{\mathcal{N}}^{\frac{3}{2}}K^2u(0)\right\|_{\mathcal{N}}^2+C\tau\left\|\Delta_{\mathcal{N}}^{\frac{3}{2}}K\hat{f}(u(0))\right\|_{\mathcal{N}}^2\\
&\le C\tau\left\|\Delta_{\mathcal{N}}^{\frac{3}{2}}(I-A\tau^3\Delta_{\mathcal{N}}^3)^{-2}\Delta_{\mathcal{N}}^4u(0)\right\|_{\mathcal{N}}^2\le C\tau\|u(0)\|_{H_h^{11}}^2.
\end{aligned}\tag{74}$$

Therefore, combining (71)–(73) and using Lemma 5 gives

$$\frac{\mathrm{d}\omega(t)}{\mathrm{d}t}\le\frac{3}{2\tau}\omega(t)+C\tau^5+\left(\frac{27}{2\varepsilon^2}+27\tau\right)\sum_{i=1}^{3}\|\nabla_{\mathcal{N}}\mathcal{R}_i(0)\|_{\mathcal{N}}^2+3\tau\sum_{i=1}^{3}\|\mathcal{R}_i(t)\|_{\mathcal{N}}^2. \tag{75}$$

Multiplying both sides by $e^{-\frac{3t}{2\tau}}$ and integrating from 0 to τ, using (40) and $\omega(0) = 0$, one gets

$$\omega(t_1) \le C\tau^6 + \left(\frac{27}{2\varepsilon^2} + 27\tau\right)\sum_{i=1}^{3}\|\nabla_{\mathcal{N}}\mathcal{R}_i(0)\|^2_{L^2(I_{0,1};\ell^2)} + 3\tau\sum_{i=1}^{3}\|\mathcal{R}_i(t)\|^2_{L^2(I_{0,1};\ell^2)}$$
$$\le C(\tau^6 + h^{2m}). \tag{76}$$

This completes the proof of the lemma. □

Below is the main result of this section.

Theorem 2 *Assume that the exact solution satisfies the regularity*

$$u_e \in H^1(0,T;H^{m+7}_{per}(\Omega)) \cap H^2(0,T;H^3_{per}(\Omega))$$
$$\cap W^{2,\infty}(0,T;H^2_{per}(\Omega)) \cap H^3(0,T;H^2_{per}(\Omega)).$$

Define $u(t) := u_e(t)|_{\Omega_{\mathcal{N}}}$ and denote by $\{u_s^n\}_{n=0}^{N_t}$ the numerical solution of (11) with $u_s^0 = u(0) \in H_h^{11}(\Omega)$. If $\tau < \frac{1}{16}$, $h < 1$, one gets

$$\|u(t_n) - u_s^n\|_{\mathcal{N}} \le C(\tau^3 + N^{-m}), \quad 1 \le n \le N_t, \tag{77}$$

with $C > 0$ independent on the time step size τ and the spatial discretization parameter N.

Proof Define the error function $e(t) = u(t) - u_s^{n+1}(t) \in \mathcal{M}^{\mathcal{N}}$. Denote $u_e(t_n)$ and $u(t_n)$ as u_e^n and u^n, respectively. Subtracting (6) from (1), one gets: for $t_2 \le t \le t_{n+1}$,

$$\frac{\mathrm{d}e(t)}{\mathrm{d}t} - A\tau^3\frac{\mathrm{d}\Delta^3_{\mathcal{N}}e(t)}{\mathrm{d}t} + \varepsilon^2\Delta^2_{\mathcal{N}}e(t)$$
$$= -\sum_{i=0}^{2}\ell_i(t-t_n)\nabla_{\mathcal{N}}\cdot\left[\beta(\nabla_{\mathcal{N}}u^{n-i}) - \beta(\nabla_{\mathcal{N}}u_s^{n-i})\right] + \mathcal{R}(t), \tag{78}$$

in which $\mathcal{R}(t) = \sum_{i=1}^4\mathcal{R}_i(t)$, with $\sum_{i=1}^3\mathcal{R}_i(t)$ defined as in (31)–(32), and

$$\mathcal{R}_4(t) = \sum_{i=0}^{2}\ell_i(t-t_n)\nabla_{\mathcal{N}}\cdot\beta(\nabla_{\mathcal{N}}u^{n-i}) - \nabla_{\mathcal{N}}\cdot\beta(\nabla_{\mathcal{N}}u(t)). \tag{79}$$

Taking the inner product with $e(t)$ on both sides of (78), one gets:

$$\frac{1}{2}\frac{\mathrm{d}\|e(t)\|^2_{\mathcal{N}}}{\mathrm{d}t} + \frac{A\tau^3}{2}\frac{\mathrm{d}\|\nabla_{\mathcal{N}}\Delta_{\mathcal{N}}e(t)\|^2_{\mathcal{N}}}{\mathrm{d}t} + \varepsilon^2\|\Delta_{\mathcal{N}}e(t)\|^2_{\mathcal{N}}$$
$$= \sum_{i=0}^{2}\ell_i(t-t_n)\left(\beta(\nabla_{\mathcal{N}}u^{n-i}) - \beta(\nabla_{\mathcal{N}}u_s^{n-i}), \nabla_{\mathcal{N}}e(t)\right)_{\mathcal{N}} + (\mathcal{R}(t), e(t))_{\mathcal{N}}$$
$$:= (\mathrm{NL}) + (\mathcal{R}(t), e(t))_{\mathcal{N}}. \tag{80}$$

The truncation error term could be bounded by the Cauchy–Schwarz inequality:

$$(\mathcal{R}(t), e(t))_{\mathcal{N}} \le \frac{\|\mathcal{R}(t)\|^2_{\mathcal{N}}}{2} + \frac{\|e(t)\|^2_{\mathcal{N}}}{2}. \tag{81}$$

An application of Lemmas 5 and 6 (with $\lambda_1 = \frac{1}{8}, \lambda_2 = \frac{1}{2}$ to (NL)) results in

$$(\mathrm{NL}) \leq C(1+h)\left(\frac{2}{\varepsilon^2}+\frac{1}{2}\right)\sum_{i=0}^{2}\|e(t_{n-i})\|_{\mathcal{N}}^2 + \frac{7\varepsilon^2}{8}\|\Delta_{\mathcal{N}} e(t)\|_{\mathcal{N}}^2 + \frac{7}{2}\|e(t)\|_{\mathcal{N}}^2, \tag{82}$$

where C only depends on $\|u(0)\|_{H_h^6}$ and $\Omega_{\mathcal{N}}$.

A substitution of (81) and (82) into (80) yields

$$\begin{aligned}
&\frac{1}{2}\frac{\mathrm{d}\|e(t)\|_{\mathcal{N}}^2}{\mathrm{d}t} + \frac{A\tau^3}{2}\frac{\mathrm{d}\|\nabla_{\mathcal{N}}\Delta_{\mathcal{N}} e(t)\|_{\mathcal{N}}^2}{\mathrm{d}t} + \frac{\varepsilon^2}{8}\|\Delta_{\mathcal{N}} e(t)\|_{\mathcal{N}}^2 \\
&\quad \leq C(1+h)\left(\frac{2}{\varepsilon^2}+\frac{1}{2}\right)\sum_{i=0}^{2}\|e(t_{n-i})\|_{\mathcal{N}}^2 + 4\|e(t)\|_{\mathcal{N}}^2 + \frac{\|\mathcal{R}(t)\|_{\mathcal{N}}^2}{2}.
\end{aligned}\tag{83}$$

Denote $\omega(t) = \frac{1}{2}\|e(t)\|_{\mathcal{N}}^2 + \frac{A\tau^3}{2}\|\nabla_{\mathcal{N}}\Delta_{\mathcal{N}} e(t)\|_{\mathcal{N}}^2$. Multiplying both sides by e^{-8t} gives

$$\frac{\mathrm{d}}{\mathrm{d}t}e^{-8t}\omega(t) \leq \left[C(1+h)\left(\frac{2}{\varepsilon^2}+\frac{1}{2}\right)\sum_{i=0}^{2}\|e(t_{n-i})\|_{\mathcal{N}}^2 + \frac{\|\mathcal{R}(t)\|_{\mathcal{N}}^2}{2}\right]e^{-8t}. \tag{84}$$

Integrating (84) from t_n to t_{n+1} and multiplying both sides by e^{8t_n}, one gets

$$\begin{aligned}
&e^{-8\tau}\omega(t_{n+1}) - \omega(t_n) \\
&\quad \leq \frac{1-e^{-8\tau}}{8}C(1+h)\left(\frac{2}{\varepsilon^2}+\frac{1}{2}\right)\sum_{i=0}^{2}\|e(t_{n-i})\|_{\mathcal{N}}^2 + \|\mathcal{R}(t)\|_{L^2(I_{n,n+1};\ell^2)}^2.
\end{aligned}\tag{85}$$

Furthermore, since $e^x \geq 1 + x$ for $x \in \mathbb{R}$, it is observed that

$$\begin{aligned}
&\omega(t_{n+1}) - \omega(t_n) - 8\tau\omega(t_{n+1}) \\
&\quad \leq C(1+h)\tau\left(\frac{2}{\varepsilon^2}+\frac{1}{2}\right)\sum_{i=0}^{2}\|e(t_{n-i})\|_{\mathcal{N}}^2 + \sum_{i=1}^{4}\|R_i(t)\|_{L^2(I_{n,n+1};\ell^2)}^2.
\end{aligned}\tag{86}$$

As for $\mathcal{R}_4(t)$, note that

$$\mathcal{R}_4(t) = \sum_{i=0}^{2}\ell_i(t-t_{n-i})\int_t^{t_{n-i}}(t_{n-i}-s)^2\partial_{ttt}(\nabla_{\mathcal{N}}\cdot\beta(\nabla_{\mathcal{N}} u(s)))\,\mathrm{d}s. \tag{87}$$

Applying Hölder's inequality and (5) implies that

$$\|\mathcal{R}_4(t)\|_{\mathcal{N}} \leq C\tau^{\frac{5}{2}}\|\nabla_{\mathcal{N}}\cdot\beta(\nabla_{\mathcal{N}} u(t))\|_{H^3(I_{n-1,n+1};\ell^2)} \leq C\tau^{\frac{5}{2}}\|u_e(t)\|_{H^3(I_{n-1,n+1};H^2)}. \tag{88}$$

Recalling the estimates of $\mathcal{R}_1 \sim \mathcal{R}_3$ in (37)–(39), one arrives at

$$\begin{aligned}
&\sum_{i=1}^{4}\|R_i(t)\|_{L^2(I_{n,n+1};\ell^2)}^2 \\
&\quad \leq C(h^{2m}+\tau^6)\left[\|u_e(t)\|_{H^1(I_{n,n+1};H^{m+6})} + \|u_e(t)\|_{H^3(I_{n-1,n+1};H^2)}^2\right].
\end{aligned}$$

A substitution of the above estimates into (86) and summing up from 2 to n implies that

$$\omega(t_{n+1})-\omega(t_2)-8\tau\sum_{i=2}^{n+1}\omega(t_i)\le C(1+h)\tau\left(\frac{2}{\varepsilon^2}+\frac{1}{2}\right)\sum_{i=0}^{n}\|e(t_i)\|_{\mathcal{N}}^2+C(h^{2m}+\tau^6),$$

where C depends on $\|u_e\|_{H^1(0,T;H^{m+6})}$ and $\|u_e\|_{H^3(0,T;H^2)}$. Since $8\tau<\frac{1}{2}$, one gets

$$\omega(t_{n+1})\le C(1+h)\left(\frac{1}{\varepsilon^2}+1\right)\tau\sum_{i=0}^{n}\omega(t_i)+C(h^{2m}+\tau^6)+C\omega(t_2). \tag{89}$$

As for $\omega(t_2)$, because of the fact that $u_s^0=u_0$, for $t_1\le t\le t_2$, one gets

$$\begin{aligned}&\frac{\mathrm{d}e(t)}{\mathrm{d}t}+A\tau^3\frac{\mathrm{d}\Delta_{\mathcal{N}}^3e(t)}{\mathrm{d}t}+\varepsilon^2\Delta_{\mathcal{N}}^2e(t)\\&\quad=-\frac{t}{\tau}\nabla_{\mathcal{N}}\cdot\left[\beta(\nabla_{\mathcal{N}}u^1)-\beta(\nabla_{\mathcal{N}}u_s^1)\right]+\sum_{i=1}^{3}\mathcal{R}_i(t)+\mathcal{R}_{4,2}(t),\end{aligned} \tag{90}$$

where $\sum_{i=1}^{3}\mathcal{R}_i(t)$ are defined in (31)–(32), $\mathcal{R}_{4,2}(t)$ is defined in (43).

Similar to (83), one gets

$$\begin{aligned}&\frac{1}{2}\frac{\mathrm{d}\|e(t)\|_{\mathcal{N}}^2}{\mathrm{d}t}+\frac{A\tau^3}{2}\frac{\mathrm{d}\|\nabla_{\mathcal{N}}\Delta_{\mathcal{N}}e(t)\|_{\mathcal{N}}^2}{\mathrm{d}t}+\frac{3\varepsilon^2}{4}\|\Delta_{\mathcal{N}}e(t)\|_{\mathcal{N}}^2\\&\quad\le C(1+h)\left(\frac{2}{\varepsilon^2}+\frac{1}{2}\right)\|e(t_1)\|_{\mathcal{N}}^2+\left(1+\frac{1}{2\tau}\right)\|e(t)\|_{\mathcal{N}}^2\\&\qquad+\sum_{i=1}^{3}\frac{\|\mathcal{R}_i(t)\|_{\mathcal{N}}^2}{2}+\frac{\tau}{2}\|\mathcal{R}_{4,2}(t)\|_{\mathcal{N}}^2.\end{aligned} \tag{91}$$

Repeating the analyses as in (84)–(85), one arrives at

$$\omega(t_2)\le e^{2\tau+1}\left[\omega(t_1)+C(1+h)\left(\frac{1}{\varepsilon^2}+1\right)\tau\|e(t_1)\|_{\mathcal{N}}^2+C(h^{2m}+\tau^6)\right], \tag{92}$$

where C also depends on $\|u_e\|_{W^{2,\infty}(0,T;H^2)}$.

A substitution of Lemma 7 and (92) into (89) results in

$$\frac{1}{2}\omega(t_{n+1})\le\left[C(1+h)\left(\frac{2}{\varepsilon^2}+\frac{1}{2}\right)+8\right]\tau\sum_{i=0}^{n}\omega(t_i)+C(h^{2m}+\tau^6). \tag{93}$$

An application of the discrete Gronwall's inequality yields the desired convergence result, $\omega(t_{n+1})\le C(h^{2m}+\tau^6)$, i.e.,

$$\|e(t_{n+1})\|_{\mathcal{N}}^2+A\tau^2\|\Delta_{\mathcal{N}}e(t_{n+1})\|_{\mathcal{N}}^2\le C(h^{2m}+\tau^6), \tag{94}$$

where C is independent of h and τ. □

Remark 4.1 We have taken the artificial dissipation term of the form of $A\tau^k \frac{\partial(\Delta_{\mathcal{N}}^2)^{p(k)}u(t)}{\partial t}$ with $p(k) = k/2$ for schemes of order k in time. The value of $p(k)$ plays a very important role in the energy stability and in the convergence property for the numerical scheme, both at theoretical and numerical values. For instance, to obtain a third-order temporal accuracy, $p(3) = \frac{3}{2}$ turns out to be a critical value to theoretically preserve the energy stability with an $\mathcal{O}(1)$ artificial regularization coefficient A. In fact, the Lipschitz condition on the nonlinear term gives (22)–(23), due to which we roughly need to control $\tau \frac{\mathrm{d}\Delta_{\mathcal{N}} u}{\mathrm{d}t}$ with the aid of the dissipation terms $A\tau^3 \frac{\mathrm{d}}{\mathrm{d}t}(-\Delta_{\mathcal{N}})^{2p(3)}u$ and $\frac{\mathrm{d}u}{\mathrm{d}t}$, then $p(3) = \frac{3}{2}$ is the choice that makes A of $\mathcal{O}(1)$ magnitude. If the power index is taken to be $p(3) < \frac{3}{2}$, such as $p = 1$ as in an existing work [14], an energy stability has been proved with $A = \mathcal{O}(\varepsilon^{-2})$. In this case, the artificial diffusion power has been reduced, while the corresponding coefficient has been drastically increased, which may lead to much larger truncation error, while the temporal accuracy order is kept unchanged. If the power index is taken to be $p(3) > \frac{3}{2}$, the theoretical justification of both the energy stability and third-order convergence analysis remains valid, with the artificial regularization coefficient $A = \mathcal{O}(1)$; on the other hand, the truncation error is expected to be larger than the one with the critical power index $p(3) = \frac{3}{2}$, especially for high frequency part, although the temporal accuracy order is still kept as the third order. Because of these two considerations, we take the critical value of the artificial regularization $p(3) = \frac{3}{2}$, for the sake of both the theoretical property and numerical performance.

The convergence test results for five difference values of p: $p = 1$, $p = 1.4$, $p = 1.6$, $p = \frac{3}{2}$ and $p = 2$ are presented in the next section, as illustrated in Tables 1, 2 and 3, respectively. It is observed that, the proposed scheme preserves very nice third-order temporal convergence rates with a refined time step size, with all these values of $p(3)$ and an $\mathcal{O}(1)$ artificial regularization coefficient A. In fact, for all these choices of $p(3)$ and A, the optimal rate convergence analysis is always available. And also, an $\mathcal{O}(\varepsilon^{-2})$ requirement for A in the case of $p = 1$ in the energy stability analysis turns out to be a theoretical issue; the energy dissipation has always been observed in the practical computations even for $p = 1$ and $A = \mathcal{O}(1)$ case. We also observe that the errors increase as the power index $p(k)$ increases, consistent with our intuition that stronger artificial dissipation leads to larger errors.

5 Numerical results

5.1 Temporal convergence of sETDMs3

In this section, we test the temporal convergence of sETDMs3. Let $\Omega = [0, 2\pi]^2$, $\varepsilon^2 = 0.01$, $T = 1$, $N = 128$, $A = \frac{1}{2\alpha^3}$ with α defined as in (18). With an additional time-dependent forcing term, we set the exact solution to be $u_e(t) = e^{-t}\cos(2x)\cos(2y)$. Also, consider three different ways to compute u_s^1, namely using the exact value, a_s^1 or as in (8). For this exact profile, a careful calculation gives

$$
\begin{aligned}
g = {} & (-1 + 64\varepsilon^2)u - \frac{8u}{1 + 2e^{-2t}[1 - \cos(4x)\cos(4y)]} \\
& + \frac{16e^{-2t}u}{[1 + 2e^{-2t}(1 - \cos(4x)\cos(4y))]^2}[\cos(4x) + \cos(4y) - 2\cos(4x)\cos(4y)].
\end{aligned}
$$

Table 1 Temporal convergence of sETDMs3 ($u_e(t) = e^{-t}\cos(2x)\cos(2y)$, $p(3) = 3/2$)

τ	$u_s^1 = a_s^1$		$u_s^1 = u^1$		u_s^1 by (8)	
	Error	Order	Error	Order	Error	Order
2.50E−03	1.25E−04		1.37E−04	0.000	1.38E−04	0.000
1.25E−03	1.40E−05	3.152	1.72E−05	2.993	1.73E−05	2.995
6.25E−04	1.35E−06	3.375	2.16E−06	2.998	2.16E−06	2.999
3.13E−04	7.01E−08	4.271	2.70E−07	2.999	2.70E−07	3.000
1.56E−04	1.71E−08	2.032	3.37E−08	3.000	3.37E−08	3.000
7.81E−05	8.43E−09	1.022	4.22E−09	3.000	4.22E−09	3.000
3.91E−05	2.63E−09	1.682	5.31E−10	2.988	5.32E−10	2.988
1.95E−05	7.25E−10	1.857	6.62E−11	3.005	6.62E−11	3.005

Table 2 Temporal convergence of sETDMs3 ($u_e(t) = e^{-t}\cos(2x)\cos(2y)$, $p(3) = 1.4$)

τ	$u_s^1 = a_s^1$		$u_s^1 = u^1$		u_s^1 by (8)	
	Error	Order	Error	Order	Error	Order
2.50E−03	6.06E−05		7.33E−05		7.36E−05	
1.25E−03	5.99E−06	3.340	9.20E−06	2.994	9.22E−06	2.996
6.25E−04	3.51E−07	4.092	1.15E−06	2.998	1.15E−06	2.999
3.13E−04	5.98E−08	2.554	1.44E−07	2.999	1.44E−07	3.000
1.56E−04	3.26E−08	0.874	1.80E−08	3.000	1.80E−08	3.000
7.81E−05	1.04E−08	1.651	2.25E−09	3.001	2.25E−09	3.001
3.91E−05	2.88E−09	1.851	2.79E−10	3.012	2.79E−10	3.012
1.95E−05	7.60E−10	1.923	3.35E−11	3.057	3.35E−11	3.057

Table 3 Temporal convergence of sETDMs3 ($u_e(t) = e^{-t}\cos(2x)\cos(2y)$, $p(3) = 1.6$)

τ	$u_s^1 = a_s^1$		$u_s^1 = u^1$		u_s^1 by (8)	
	Error	Order	Error	Order	Error	Order
2.50E−03	1.56E−04		1.68E−04		1.69E−04	0.000
1.25E−03	1.79E−05	3.119	2.11E−05	2.992	2.12E−05	2.994
6.25E−04	1.84E−06	3.285	2.64E−06	2.998	2.65E−06	2.999
3.13E−04	1.30E−07	3.821	3.31E−07	2.999	3.31E−07	3.000
1.56E−04	9.88E−09	3.721	4.13E−08	3.000	4.14E−08	3.000
7.81E−05	7.49E−09	0.399	5.17E−09	3.000	5.17E−09	3.000
3.91E−05	2.52E−09	1.574	6.44E−10	3.003	6.45E−10	3.003
1.95E−05	7.20E−10	1.805	7.16E−11	3.171	7.16E−11	3.171

Results for $p(3) = \frac{3}{2}$, $p(3) = 1.4$, $p(3) = 1.6$, $p(3) = 1$ and $p(3) = 2$ are shown in Tables 1, 2, 3, 4 and 5, respectively. Third-order temporal convergence rates have been observed for all these values of p, as the time step size is refined. For $p(3) = 1$, the loss of accuracy in the last row is due, perhaps, to rounding errors.

5.2 Simulation results of coarsening process

In this subsection, we set $\Omega = [0, 12.8]^2$, $\varepsilon^2 = 0.005$, $T = 40000$, $A = \frac{1}{2\alpha^3}$ with α defined as in (18) and use a random initial data within $[-0.05, 0.05]$. We use a coarser uniform mesh with $N = 128$ and set time step size $\tau = 0.001$.

Figure 1 shows the snapshots of the numerical solution (11) at time $t = 1$, 1E4, 1.5E4, 2E4, 3E4, 4E4. It can be observed that the solution has saturated to a one-hill-one-valley structure at the final time.

Table 4 **Temporal convergence of sETDMs3 ($u_e(t) = e^{-t}\cos(2x)\cos(2y)$, $p(3) = 1$)**

τ	$u_s^1 = a_s^1$		$u_s^1 = u^1$		u_s^1 by (8)	
	Error	Order	Error	Order	Error	Order
2.50E−03	4.44E−06		1.72E−05		1.73E−05	
1.25E−03	1.10E−06	2.007	2.15E−06	2.997	2.17E−06	2.999
6.25E−04	5.41E−07	1.029	2.70E−07	2.999	2.71E−07	2.999
3.13E−04	1.69E−07	1.682	3.37E−08	2.999	3.39E−08	2.999
1.56E−04	4.63E−08	1.864	4.21E−09	3.000	4.24E−09	3.000
7.81E−05	1.21E−08	1.936	5.26E−10	3.001	5.29E−10	3.001
3.91E−05	3.10E−09	1.967	6.06E−11	3.118	6.10E−11	3.117
1.95E−05	7.93E−10	1.966	1.58E−11	1.943	1.58E−11	1.951

Table 5 **Temporal convergence of sETDMs3 ($u_e(t) = e^{-t}\cos(2x)\cos(2y)$, $p(3) = 2$)**

τ	$u_s^1 = a_s^1$		$u_s^1 = u^1$		u_s^1 by (8)	
	Error	Order	Error	Order	Error	Order
2.50E−03	9.62E−04		9.70E−04		9.73E−04	0.000
1.25E−03	1.31E−04	2.877	1.34E−04	2.857	1.34E−04	2.859
6.25E−04	1.64E−05	2.999	1.72E−05	2.963	1.72E−05	2.964
3.13E−04	1.96E−06	3.067	2.16E−06	2.994	2.16E−06	2.995
1.56E−04	2.19E−07	3.156	2.70E−07	2.999	2.70E−07	2.999
7.81E−05	2.11E−08	3.375	3.37E−08	3.000	3.37E−08	3.000
3.91E−05	1.10E−09	4.270	4.21E−09	3.000	4.21E−09	3.000
1.95E−05	2.60E−10	2.077	5.35E−10	2.977	5.35E−10	2.977

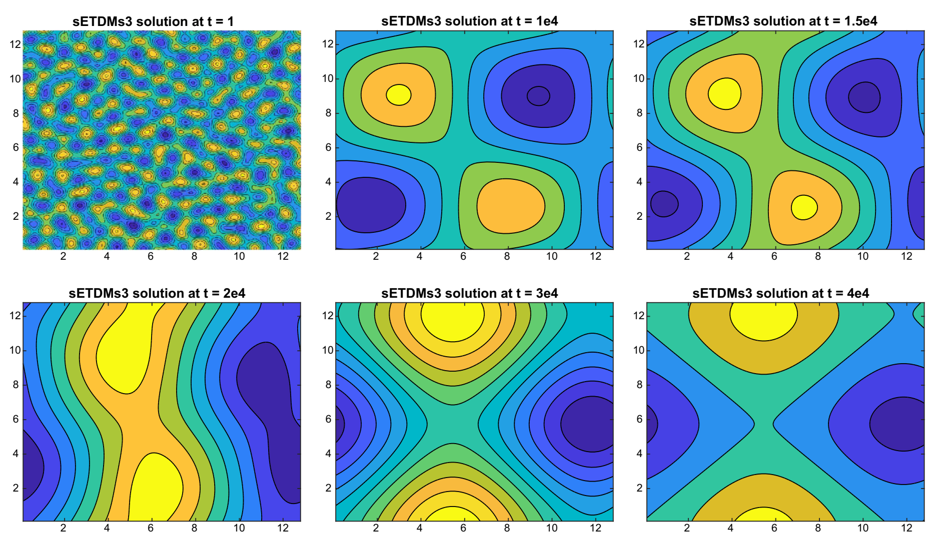

Fig. 1 Snapshots of the numerical solutions

Recall the discrete energy functional in (17), for convenience we repeat it here:

$$E_{\mathcal{N}}(u) = \left(-\frac{1}{2}\ln(1 + |\nabla_{\mathcal{N}} u|^2), 1\right)_{\mathcal{N}} + \frac{\varepsilon^2}{2}\|\Delta_{\mathcal{N}} u\|_{\mathcal{N}}^2, \quad \forall u \in \mathcal{M}^{\mathcal{N}}. \tag{95}$$

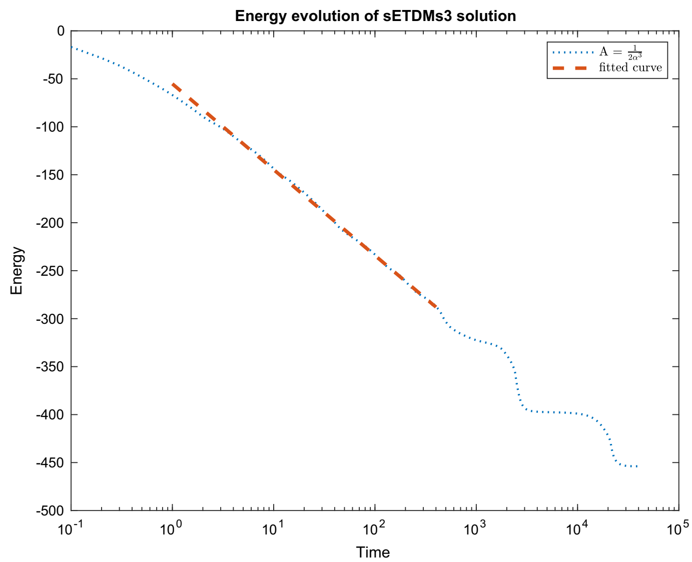

Fig. 2 Semi-log plot of the energy $E_{\mathcal{N}}$ of sETDMs3. Fitted line has the form $a\ln(t) + b$, with coefficients $a = -38.85$, $b = -55.24$

Also, consider the average surface roughness $h_{\mathcal{N}}(u)$ and the average slope $m_{\mathcal{N}}(u)$:

$$h_{\mathcal{N}}(u,t) = \sqrt{\frac{h^2}{|\Omega|}\sum_{\mathcal{M}^{\mathcal{N}}}|u(\mathbf{x}_{i,j},t) - \bar{u}(t)|^2}, \quad \text{with} \quad \bar{u}(t) := \frac{h^2}{|\Omega|}\sum_{\mathcal{M}^{\mathcal{N}}} u(\mathbf{x}_{i,j},t). \tag{96}$$

$$m_{\mathcal{N}}(u,t) = \sqrt{\frac{h^2}{|\Omega|}\sum_{\mathcal{M}^{\mathcal{N}}}|\nabla u(\mathbf{x}_{i,j},t)|^2}. \tag{97}$$

For the no-slope-selection growth model (1), recall that $E_{\mathcal{N}} \sim O(-\ln(t))$, $h_{\mathcal{N}} \sim O(t^{\frac{1}{2}})$ and $m_{\mathcal{N}} \sim O(t^{\frac{1}{4}})$ as $t \to \infty$ (see [24,38,39] and references therein). The evolution of $E_{\mathcal{N}}$, $h_{\mathcal{N}}$ and $m_{\mathcal{N}}$ is demonstrated in Figs. 2 and 3, respectively. The linear fitting results for the solution of sETDMs3 in time interval $[1, 400]$ are also presented in corresponding figures. The evolution of the discrete energy for the case of $p(3) = 1$ with the same regularization coefficient A as in the case of $p(3) = 3/2$ is illustrated in Fig. 4. The difference in numerical results is small indicating the performance of the scheme is insensitivity of the value of $p(k)$ despite the theoretical requirement.

We also observe that the errors increase as the power index $p(k)$ increases, consistent with our intuition that stronger artificial dissipation leads to larger errors.

6 Concluding remarks

We have introduced a strategy for designing higher-order in time, energy stable linear numerical schemes by combining ETD method , multi-step method and a higher-order continuous Dupont–Douglas type regularization for gradient flows with mild nonlinearity. As an example, a linear, third order in time accurate, energy stable ETD-based scheme for a thin film model without slope selection is presented. An unconditional long-time energy stability is justified at a theoretical level. In addition, an $O(\tau^3)$-order convergence analysis is established in the $\ell^\infty(0,T;\ell^2)$ norm. Moreover, various numerical experiments have

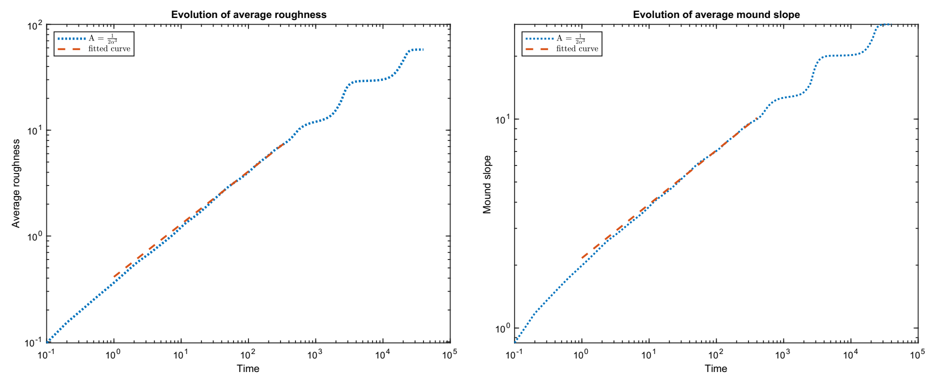

Fig. 3 The log–log plot of (1) the average surface roughness $h_{\mathcal{N}}$ and (2) the average slope $m_{\mathcal{N}}$ of sETDMs3. Fitted lines have the form at^b, with coefficients (1) $a = 0.4113$, $b = 0.4983$ and (2) $a = 2.162$, $b = 0.2578$

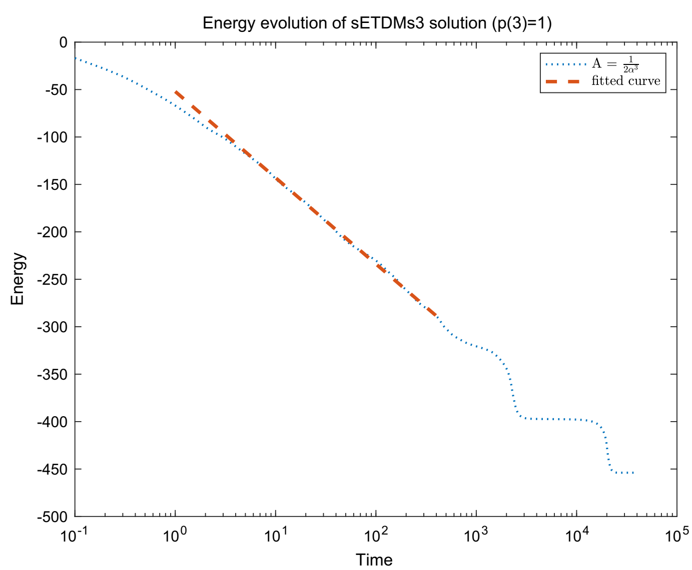

Fig. 4 Semi-log plot of the energy $E_{\mathcal{N}}$ of sETDMs3 with $p(3) = 1$. Fitted line has the form $a\ln(t) + b$, with coefficients $a = -39.48$, $b = -52.04$

demonstrated that the proposed third-order scheme is able to produce accurate long-time numerical results with a reasonable computational cost.

Acknowledgements
This work is supported in part by the Grants NSFC 11671098, 91630309, a 111 Project B08018 (W. Chen), NSF DMS-1418689 (C. Wang), NSFC11871159, Guangdong Provincial Key Laboratory for Computational Science and Material Design 2019B030301001 (X. Wang). C. Wang also thanks the Key Laboratory of Mathematics for Nonlinear Sciences, Fudan University, for support during his visit.

Author details
[1]Shanghai Key Laboratory of Mathematics for Nonlinear Sciences, School of Mathematical Sciences, Fudan University, Shanghai 200433, People's Republic of China, [2]School of Mathematical Sciences, Fudan University, Shanghai 200433, People's Republic of China, [3]Mathematics Department, University of Massachusetts, North Dartmouth, MA 02747, USA, [4]SUSTech International Center for Mathematics and Department of Mathematics, Southern University of Science and Technology, Shenzhen 518055, People's Republic of China.

Received: 22 February 2020 Accepted: 15 June 2020
Published online: 29 June 2020

References

1. Abramov, R., Majda, A.J.: Blended response algorithms for linear fluctuation-dissipation for complex nonlinear dynamical system. Nonlinearity **20**(12), 2793–2822 (2007)
2. Adams, R.A., Fournier, J.J.F.: Sobolev Spaces. Academic press, Singapore (2003)
3. Benesova, B., Melcher, C., Suli, E.: An implicit midpoint spectral approximation of nonlocal Cahn–Hilliard equations. SIAM J. Numer. Anal. **52**, 1466–1496 (2014)
4. Beylkin, G., Keiser, J.M., Vozovoi, L.: A new class of time discretization schemes for the solution of nonlinear PDEs. J. Comput. Phys. **147**, 362–387 (1998)
5. Canuto, C., Hussaini, M.Y., Quarteroni, A., Zang, T.A.: Spectral Methods: Fundamentals in Single Domains. Springer, Berlin (2006)
6. Canuto, C., Hussaini, M.Y., Quarteroni, A., Zang, T.A.: Spectral Methods: Evolution to Complex Geometries and Applications to Fluid Dynamics. Springer, Berlin (2007)
7. Canuto, C., Quarteroni, A.: Approximation results for orthogonal polynomials in sobolev spaces. Math. Comp. **38**, 67–86 (1982)
8. Chen, W., Conde, S., Wang, C., Wang, X., Wise, S.M.: A linear energy stable scheme for a thin film model without slope selection. J. Sci. Comput. **52**, 546–562 (2012)
9. Chen, W., Li, W., Luo, Z., Wang, C., Wang, X.: A stabilized second order exponential time differencing multistep method for thin film growth model without slope selection. ESAIM: M2AN **54**(3), 727–750 (2020)
10. Chen, W., Wang, C., Wang, X., Wise, S.M.: A linear iteration algorithm for a second-order energy stable scheme for a thin film model without slope selection. J. Sci. Comput. **59**, 574–601 (2014)
11. Chen, W., Wang, X., Yan, Y., Zhang, Z.: A second order BDF numerical scheme with variable steps for the Cahn–Hilliard equation. SIAM Numer. Anal. **57**, 495–525 (2019)
12. Chen, W., Wang, Y.: A mixed finite element method for thin film epitaxy. Numer. Math. **122**, 771–793 (2012)
13. Cheng, K., Feng, W., Wang, C., Wise, S.M.: An energy stable fourth order finite difference scheme for the Cahn–Hilliard equation. J. Comput. Appl. Math. **362**, 574–595 (2019)
14. Cheng, K., Qiao, Z., Wang, C.: A third order exponential time differencing numerical scheme for no-slope-selection epitaxial thin film model with energy stability. J. Sci. Comput. **81**, 154–185 (2019)
15. Cheng, K., Wang, C., Wise, S.M.: An energy stable Fourier pseudo-spectral numerical scheme for the square phase field crystal equation. Commu. Comput. Phys. **26**, 1335–1364 (2019)
16. Cheng, Q., Shen, J., Yang, X.: Highly efficient and accurate numerical schemes for the epitaxial thin film growth models by using the SAV approach. J. Sci. Comput. **78**, 1467–1487 (2019)
17. Cox, S.M., Matthews, P.C.: Exponential time differencing for stiff systems. J. Comput. Phys. **176**, 430–455 (2002)
18. Ehrlich, G., Hudda, F.G.: Atomic view of surface self-diffusion: tungsten on tungsten. J. Chem. Phys. **44**, 1039–1049 (1966)
19. Engquist, B., Majda, A.: Radiation boundary conditions for acoustic and elastic wave calculations. Commun. Pure Appl. Math. **32**, 313–357 (1979)
20. Eyre, D.J.: Unconditionally gradient stable time marching the Cahn–Hilliard equation. In: MRS Online Proceedings Library Archive, Volume 529 (Symposia BB–Computational & Mathematical Models of Microstructural Evolution), p. 39 (1998)
21. Feng, K., Qin, M.: Symplectic Geometric Algorithms for Hamiltonian Systems. Springer, Berlin (2010)
22. Feng, W., Wang, C., Wise, S.M., Zhang, Z.: A second-order energy stable backward differentiation formula method for the epitaxial thin film equation with slope selection. Numer. Methods Part. Differ. Equ. **34**, 1975–2007 (2018)
23. Feng, X., Tang, T., Yang, J.: Long time numerical simulations for phase-field problems using p-adaptive spectral deferred correction methods. SIAM J. Sci. Comput. **37**, A271–A294 (2015)
24. Golubović, L.: Interfacial coarsening in epitaxial growth models without slope selection. Phys. Rev. Lett. **78**, 90–93 (1997)
25. Gottlieb, D., Orszag, S.A.: Numerical Analysis of Spectral Methods: Theory and Applications. SIAM, Philadelphia (1977)
26. Gottlieb, S., Shu, C.W., Tadmor, E.: Strong stability-preserving high-order time discretization methods. SIAM Rev. **43**, 89–112 (2001)
27. Gottlieb, S., Wang, C.: Stability and convergence analysis of fully discrete fourier collocation spectral method for 3-D viscous Burgers' equation. J. Sci. Comput. **53**, 102–128 (2012)
28. Hairer, E., Noersett, S.P., Wanner, G.: Solving Ordinary Differential Equations I: Nonstiff Problems. Springer, Berlin (1987)
29. Hochbruck, M., Ostermann, A.: Exponential integrators. Acta Numer. **19**, 209–286 (2010)
30. Hochbruck, M., Ostermann, A.: Exponential multistep methods of Adams-type. BIT Numer. Math. **51**, 889–908 (2011)
31. Jin, S.: Efficient asymptotic-preserving (AP) schemes for some multiscale kinetic equations. SIAM J. Sci. Comput. **21**, 441–454 (1999)
32. Ju, L., Li, X., Qiao, Z., Zhang, H.: Energy stability and error estimates of exponential time differencing schemes for the epitaxial growth model without slope selection. Math. Comput. **87**, 1859–1885 (2017)
33. Ju, L., Liu, X., Leng, W.: Compact implicit integration factor methods for a family of semilinear fourth-order parabolic equations. Discrete Contin. Dyn. Syst. B **19**, 1667–1687 (2014)
34. Ju, L., Zhang, J., Du, Q.: Fast and accurate algorithms for simulating coarsening dynamics of Cahn–Hilliard equations. Comput. Mater. Sci. **108**, 272–282 (2015)
35. Ju, L., Zhang, J., Zhu, L., Du, Q.: Fast explicit integration factor methods for semilinear parabolic equations. J. Sci. Comput. **62**, 431–455 (2015)
36. Kohn, R.V., Yan, X.: Upper bound on the coarsening rate for an epitaxial growth model. Commun. Pure Appl. Math. **56**, 1549–1564 (2003)
37. Li, B.: High-order surface relaxation versus the Ehrlich–Schwoebel effect. Nonlinearity **19**, 2581–2603 (2006)
38. Li, B., Liu, J.: Thin film epitaxy with or without slope selection. Eur. J. Appl. Math. **14**, 713–743 (2003)
39. Li, B., Liu, J.: Epitaxial growth without slope selection: energetics, coarsening, and dynamic scaling. J. Nonlinear Sci. **14**, 429–451 (2004)

40. Li, D., Qiao, Z., Tang, T.: Characterizing the stabilization size for semi-implicit Fourier-spectral method to phase field equations. SIAM J. Numer. Anal. **54**, 1653–1681 (2016)
41. Li, W., Chen, W., Wang, C., Yan, Y., He, R.: A second order energy stable linear scheme for a thin film model without slope selection. J. Sci. Comput. **76**, 1905–1937 (2018)
42. Li, X., Qiao, Z., Zhang, H.: Convergence of a fast explicit operator splitting method for the epitaxial growth model with slope selection. SIAM J. Numer. Anal. **55**, 265–285 (2017)
43. Miranville, A.: The Cahn–Hilliard Equation: Recent Advances and Applications. SIAM, Philadelphia (2019)
44. Moldovan, D., Golubovic, L.: Interfacial coarsening dynamics in epitaxial growth with slope selection. Phys. Rev. E. **61**, 6190–6214 (2000)
45. Qiao, Z., Tang, T., Xie, H.: Error analysis of a mixed finite element method for the molecular beam epitaxy model. SIAM J. Numer. Anal. **53**, 184–205 (2015)
46. Qiao, Z., Wang, C., Wise, S.M., Zhang, Z.: Error analysis of a finite difference scheme for the epitaxial thin film model with slope selection with an improved convergence constant. Int. J. Numer. Anal. Mod. **14**, 283–305 (2017)
47. Qiao, Z., Zhang, Z., Tang, T.: An adaptive time-stepping strategy for the molecular beam epitaxy models. SIAM J. Sci. Comput. **33**, 1395–1414 (2011)
48. Schwoebel, R.L.: Step motion on crystal surfaces. II. J. Appl. Phys. **40**, 614–618 (1969)
49. Shen, J., Tang, T., Wang, L.: Spectral Methods: Algorithms, Analysis and Applications. Springer, Berlin (2011)
50. Shen, J., Wang, C., Wang, X., Wise, S.M.: Second-order convex splitting schemes for gradient flows with Ehrlich–Schwoebel type energy: application to thin film epitaxy. SIAM J. Numer. Anal. **50**, 105–125 (2012)
51. Shen, J., Xu, J., Yang, J.: The scalar auxiliary variable (SAV) approach for gradient flows. J. Comput. Phys. **353**, 407–416 (2018)
52. Tam, C.K., Webb, J.C.: Dispersion-relation-preserving finite difference schemes for computational acoustics. J. Comput. Phys. **107**, 262–281 (1993)
53. Wang, C., Wang, X., Wise, S.M.: Unconditionally stable schemes for equations of thin film epitaxy. Discrete Contin. Dyn. Syst. **28**, 405–423 (2010)
54. Wang, X., Ju, L., Du, Q.: Efficient and stable exponential time differencing Runge–Kutta methods for phase field elastic bending energy models. J. Comput. Phys. **316**, 21–38 (2016)
55. Xu, C., Tang, T.: Stability analysis of large time-stepping methods for epitaxial growth models. SIAM J. Numer. Anal. **44**, 1759–1779 (2006)
56. Yang, X., Zhao, J., Wang, Q.: Numerical approximations for the molecular beam epitaxial growth model based on the invariant energy quadratization method. J. Comput. Phys. **333**, 104–127 (2017)
57. Zhu, L., Ju, L., Zhao, W.: Fast high-order compact exponential time differencing Runge–Kutta methods for second-order semilinear parabolic equations. J. Sci. Comput. **67**, 1043–1065 (2016)
58. Zhang, Z., Qiao, Z.: An adaptive time-stepping strategy for the Cahn–Hilliard equation. Commun. Comput. Phys. **11**, 1261–1278 (2012)

Publisher's Note